

Fig. 6. Evaluation of Antibody Binding Activity *in Vitro* (a: ELISA, b: Western blot). The binding specificities of the phage antibodies were assessed *in vitro* by using ELISA and Western blotting.

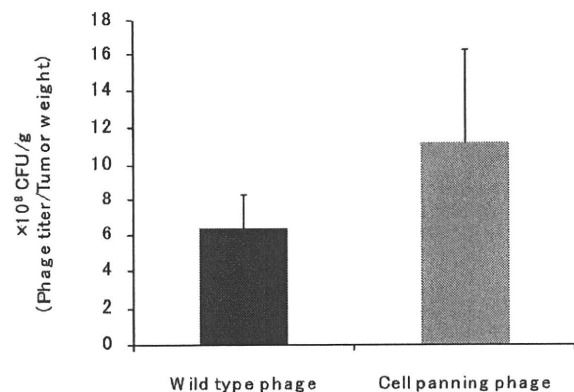


Fig. 7. Evaluation of Antibody Binding Activity in a Pilot Study *in Vivo*

The binding specificities of the phage antibodies were assessed *in vivo* by analyzing their accumulation on the tumor tissue. $n=3$, $p=0.08$.

1.8 倍の腫瘍集積性を示す傾向にあった (Fig. 7). この有意差が得られなかった原因は、抗体をファージ上に提示した状態で用いていることから、ファージが持つ非特異的吸着性の影響を受け、本来得られ

べき差異がマスクされてしまったためとわれわれは推測している。そこで今後、より詳細に獲得した抗体の抗原認識性を評価するため、得られた Clone 1 の遺伝子をもとに、抗体のみを精製し、再検討する予定である。なお、Clone 2 についても現在、同様に特性評価を行っている。

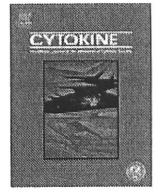
4. おわりに

本研究の結果、抗腫瘍組織血管抗体の創製に成功した。今後は免疫沈降法、質量分析法を駆使して各抗体の抗原タンパク質を同定し、それら抗原タンパク質の機能、生体分布評価を行う予定である。将来的に本研究により創製した抗体、その抗原が、がん治療、診断及び腫瘍組織血管研究の進展に大きく貢献することを期待している。

REFERENCES

- 1) Semenza G. L., *J. Clin. Invest.*, **106**, 809-812 (2000).
- 2) Yu J. L., Rak J. W., Coomber B. L., Hicklin D. J., Kerbel R. S., *Science*, **295**, 1526-1528 (2002).
- 3) Blagosklonny M. V., *Cancer Cell*, **5**, 13-17 (2004).
- 4) Klagsbrun M., Sasse J., Sullivan R., Smith J. A., *Proc. Natl. Acad. Sci. USA*, **83**, 2448-2452 (1986).
- 5) Montesano R., Vassalli J. D., Baird A., Guillemin R., Orci L., *Proc. Natl. Acad. Sci. USA*, **83**, 7297-7301 (1986).
- 6) Frater-Shroder M., Risau W., Hallmann R., Gautschi P., *Proc. Natl. Acad. Sci. USA*, **84**, 5277-5281 (1987).
- 7) Carmeliet P., *Nat. Med.*, **6**, 389-395 (2000).
- 8) Folkman J., *J. Natl. Cancer Inst.*, **82**, 4-6 (1990).
- 9) Keller R., Pratt B. M., Furthmary H., Madri J. A., *Am. J. Pathol.*, **128**, 299-306 (1987).
- 10) Aburatani H., *J. Gastroenterol.*, **40** (Suppl. 16), 1-6 (2005).
- 11) Mume E., Orlova A., Malmström P.-U., Lundqvist H., Sjöberg S., Tolmachev V., *Nucl. Med. Biol.*, **32**, 613-622 (2005).
- 12) Peknicova J., Chladek D., Hozak P., *Am. J. Reprod. Immunol.*, **53**, 42-49 (2005).
- 13) Andresen H., Grötzinger C., Zarse K., Kreuzer O. J., Ehrentreich-Förster E., Bier F. F.,

- Proteomics*, **6**, 1376–1384 (2006).
- 14) Miyata T., Jige M., Nakaminami T., Uragami T., *Proc. Natl. Acad. Sci. USA*, **103**, 1190–1193 (2006).
 - 15) O'Mahony D., Bishop M. R., *Front. Biosci.*, **11**, 1620–1635 (2006).
 - 16) Schulze-Koops H., Lipsky P. E., *Curr. Dir. Autoimmun.*, **2**, 24–49 (2000).
 - 17) Bhattacharya-Chatterjee M., Chatterjee S. K., Foon K. A., *Expert. Opin. Biol. Ther.*, **2**, 869–881 (2002).
 - 18) Takeshita A., *Rinsho Byori*, **52**, 917–923 (2004).
 - 19) González E., Gutiérrez E., Hernández Y., Roselló G., Gutiérrez M. J., Gutiérrez Martínez E., Manzanera M. J., García J. A., Praga M., Morales J. M., Andrés A., *Transplant. Proc.*, **37**, 3736–3737 (2005).
 - 20) Cheson B. D., *Cancer Immunol. Immunother.*, **55**, 188–196 (2006).
 - 21) Bohme C., *Eur. J. Oncol. Nurs.*, **4**, 30–36 (2000).
 - 22) Carter P., Fendly B. M., Lewis G. D., Sliwkowski M. X., *Breast Dis.*, **11**, 103–111 (2000).
 - 23) Murray S., *CMAJ*, **174**, 36–37 (2006).
 - 24) Kim K. J., Li B., Winter J., Armanini M., Gillett N., Phillips H. S., Ferrara N., *Nature*, **362**, 841–844 (1993).
 - 25) Presta L. G., Chen H., O'Connor S. J., Chisholm V., Meng Y. G., Krummen L., Winkler M., Ferrara N., *Cancer Res.*, **57**, 4593–4599 (1997).
 - 26) Wu N., Klitzman B., Dodge R., Dewhirst M. W., *Cancer Res.*, **52**, 4265–4268 (1992).
 - 27) Matsumura Y., Maeda H., *Cancer Res.*, **46**, 6387–6392 (1986).
 - 28) Risau W., *Nature*, **386**, 671–674 (1997).
 - 29) Ferrara N., Davis-Smyth T., *Endocr. Rev.*, **18**, 4–25 (1997).
 - 30) Shibuya M., Claesson-Welsh L., *Exp. Cell Res.*, **312**, 549–560 (2006).
 - 31) Smith G. P., *Science*, **228**, 1315–1317 (1985).
 - 32) McCafferty J., Griffiths A. D., Winter G., Chiswell D. J., *Nature*, **348**, 552–554 (1990).
 - 33) Marks J. D., Hoogenboom H. R., Bonnert T. P., McCafferty J., Griffiths A. D., Winter G., *J. Mol. Biol.*, **222**, 581–597 (1991).
 - 34) Barbas C. F. 3rd, Kang A. S., Lerner R. A., Benkovic S. J., *Proc. Natl. Acad. Sci. USA*, **88**, 7978–7982 (1991).
 - 35) Vaughan T. J., Williams A. J., Pritchard K., Osbourn J. K., Pope A. R., Earnshaw J. C., McCafferty J., Hodits R. A., Wilton J., Johnson K. S., *Nat. Biotechnol.*, **14**, 309–314 (1996).
 - 36) Coomber D. W., *Methods. Mol. Biol.*, **178**, 133–145 (2002).
 - 37) Goletz S., Christensen P. A., Kristensen P., Blohm D., Tomlinson I., Winter G., Karsten U., *J. Mol. Biol.*, **315**, 1087–1097 (2002).
 - 38) Utoguchi N., Mizuguchi H., Saeki K., Ikeda K., Tsutsumi Y., Nakagawa S., Mayumi T., *Cancer Lett.*, **89**, 7–14 (1995).
 - 39) Okamoto T., Mukai Y., Yoshioka Y., Shibata H., Kawamura M., Yamamoto Y., Nakagawa S., Kamada H., Hayakawa T., Mayumi T., Tsutsumi Y., *Biochem. Biophys. Res. Commun.*, **323**, 583–591 (2004).
 - 40) Rojas G., Almagro J. C., Acevedo B., Gavilondo J. V., *J. Biotechnol.*, **94**, 287–298 (2002).
 - 41) Zhang Z. C., Hu X. J., Yang Q., *Hepatobiliary Pancreat. Dis. Int.*, **3**, 77–81 (2004).



Generation of mouse macrophages expressing membrane-bound TNF variants with selectivity for TNFR1 or TNFR2

Hiroko Shibata^{a,b,1}, Yasuhiro Abe^{a,1}, Yasuo Yoshioka^{a,c,1}, Tetsuya Nomura^{a,d}, Masaki Sato^a, Hiroyuki Kayamuro^{a,d}, Tomoyuki Kawara^{a,d}, Shuhei Arita^{a,d}, Tsuyoshi Furuya^{a,d}, Kazuya Nagano^a, Tomoaki Yoshikawa^{a,d}, Haruhiko Kamada^{a,c}, Shin-ichi Tsunoda^{a,c,d,*}, Yasuo Tsutsumi^{a,c,d}

^a National Institute of Biomedical Innovation (NiBio), 7-6-8 Saito-Asagi, Ibaraki, Osaka 567-0085, Japan

^b National Institute of Health Science (NIHS), Kamiyoga 1-18-1, Setagaya-ku, Tokyo 158-8501, Japan

^c The Center for Advanced Medical Engineering and Informatics, Osaka University, 1-6 Yamadaoka, Suita, Osaka 565-0871, Japan

^d Graduate School of Pharmaceutical Sciences, Osaka University, 1-6 Yamadaoka, Suita, Osaka 565-0871, Japan

ARTICLE INFO

Article history:

Received 31 July 2009

Received in revised form 6 November 2009

Accepted 24 November 2009

Keywords:

Transmembrane TNF
TNFR1
TNFR2
Mutant TNF
Lentiviral vector

ABSTRACT

Tumor necrosis factor- α (TNF) is expressed on the cell surface as a transmembrane form (tmTNF), that can be released as a soluble form (solTNF) via proteolytic cleavage. These two types of TNF exert their biological functions by binding to one of two TNF receptors, TNFR1 or TNFR2. However, the biological function of tmTNF through these two receptors remains to be determined. Here, we generated macrophages that expressed tmTNF mutants with selectivity for either TNFR1 or TNFR2 as a tool to evaluate signaling through these receptors. Wild-type TNF (wtTNF), TNFR1-selective mutant TNF (mutTNF-R1) or TNFR2-selective mutant TNF (mutTNF-R2) were individually expressed on the TNFR1^{-/-}R2^{-/-} mouse macrophages (M ϕ) as the tmTNF forms. tm-mutTNF-R1-expressing M ϕ exhibited significant selectivity for binding to TNFR1, whereas tm-mutTNF-R2-expressing M ϕ only showed a slight selectivity for binding to TNFR2. Signaling by tm-mutTNF-R1-expressing M ϕ through the hTNFR2 was weaker than that of tm-wtTNF-expressing M ϕ , suggesting that the binding selectivity correlated with functional selectivity. Interestingly, signaling by tm-mutTNF-R2-expressing M ϕ through TNFR2 was much stronger than signaling by tm-wtTNF-expressing M ϕ , whereas signaling by the corresponding soluble form was weaker than that mediated by wtTNF. These results indicate tmTNF variants might prove useful for the functional analysis of signaling through TNF receptors.

© 2009 Elsevier Ltd. All rights reserved.

1. Introduction

Tumor necrosis factor alpha (TNF) plays a crucial role in the host defense system [1]. Increased secretion of TNF is involved in the development of autoimmune diseases, such as rheumatoid arthritis (RA) and Crohn's disease [2,3]. Indeed, anti-human TNF antibody and soluble TNF receptor (TNFR), which interfere with the activity of TNF, have been used to treat these diseases, and are expected to be revolutionary therapies due to their excellent therapeutic effects [4]. TNF is primarily produced as a type II transmembrane form (tmTNF) arranged in stable homotrimers [5,6]. A mature, soluble homotrimeric 17-kDa TNF (solTNF) is released from this 26 kDa memTNF via proteolytic cleavage by the metallo-

protease, TNF converting enzyme (TACE) [7]. Both solTNF and tmTNF induce cell signaling. tmTNF acts through cell–cell contacts to promote juxtacrine signaling, and solTNF acts in a paracrine fashion. The relative contribution of tmTNF and solTNF to overall TNF activity is difficult to elucidate due to the absence of physiologically relevant models. However, evidence for distinct roles for tmTNF and solTNF *in vivo* have been obtained in genetically modified mice. Study of tmTNF knock-in mice revealed that solTNF is required for the development of acute and chronic inflammation, whereas tmTNF supports many processes underlying the development of lymphoid tissue [8]. Mueller et al. also reported that tmTNF has a strong effect upon the course of cellular immune responses *in vivo* and exerts quantitatively and qualitatively distinct functions from solTNF *in vitro* and *in vivo* [9]. Additionally, juxtacrine signaling by tmTNF was shown to be essential for the resolution of inflammation and the maintenance of immunity to the pathogens, *Listeria monocytogenes* and *Mycobacterium tuberculosis* [10–12]. These different functions mediated by the two forms of TNF may help to explain the opposing activities of TNF, such as

* Corresponding author. Address: National Institute of Biomedical Innovation, Laboratory of Pharmaceutical Proteomics, 7-6-8 Saito-Asagi, Ibaraki, Osaka 567-0085, Japan. Tel.: +81 72 639 7014; fax: +81 72 641 9817.

E-mail address: tsunoda@nibio.go.jp (S.-i. Tsunoda).

¹ These authors contributed equally to this work.

its inflammatory and anti-inflammatory effects. However, the factors underlying the different functions of soluble TNF and transmembrane TNF and the components of the specific signaling cascades induced by the two forms of TNF remain to be elucidated.

soluble TNF and transmembrane TNF interact with two receptor subtypes, p55 TNF receptor (TNFR1) and p75 TNF receptor (TNFR2) [13], to exert their biological functions. The interaction of soluble TNF with TNFR and the downstream signaling and functional outcome of that signaling has been extensively studied [14], because signaling by soluble TNF via TNFR1 or TNFR2 can be analyzed *in vitro* using recombinant wild-type TNF, as well as recombinant TNFR1-, and TNFR2-selective mutant TNF (mutTNF). On the other hand, the analysis of transmembrane TNF/TNFR signaling is still poorly understood. Transmembrane TNF-expressing cells have previously been reported following transfection into target cells of a TNF gene containing a deletion of the TNF cleavage site [15]. Nanoparticles decorated with soluble TNF chemically bound to the surface initiate strong TNFR2 responses, and could mimic the bioactivity of transmembrane TNF [16]. However, there are no receptor-selective forms of transmembrane TNF that could be used to analyze transmembrane TNF/TNFR signaling. Moreover, there are few assay systems that can assess the bioactivity of TNF mediated via TNFR2 with high sensitivity.

In this context, we have used a novel phage-display based screening system to develop TNFR1 or TNFR2-selective mutant TNFs to help clarify the biology of TNF/TNFR interactions. We have already isolated a TNFR1-selective antagonist [17], and both TNFR1 and TNFR2-selective agonists [18]. Additionally, we established a novel cell line hTNFR2/mFas-preadipocyte, which is a simple and highly sensitive, cell death-based assay system for measuring TNFR2-mediated bioactivity [19]. This assay system can assess both soluble TNF and transmembrane TNF-mediated bioactivity. In this study, we first expressed the TNFR-selective mutant TNFs agonists (mutTNF-R1, mutTNF-R2) in TNFR1^{-/-}R2^{-/-} macrophages, and we then investigated the possibility of creating TNFR1- and TNFR2-selective transmembrane TNF.

2. Materials and methods

2.1. Cells

The immortalized TNFR1^{-/-}R2^{-/-} macrophage cell line (DKO M ϕ) established from the bone marrow of a TNFR1^{-/-}R2^{-/-} mouse was generously provided by Dr. Aggarwal (The University of Texas M.D. Anderson Cancer Center, Houston TX), and cultured in RPMI-1640 medium supplemented with 10% fetal bovine serum (FBS) and 1% antibiotic cocktail (penicillin 10,000 U/ml, streptomycin 10 mg/ml, and amphotericin B 25 μ g/ml; Nacalai Tesque, Kyoto, Japan). Human-TNFR2/mouse-Fas-expressing preadipocytes (hTNFR2/mFas-PA) were maintained in Dulbecco's modified Eagle's medium (DMEM; Sigma-Aldrich, Inc., Tokyo, Japan) with 10% FBS, 1% antibiotic cocktail, and 5 μ g/ml blasticidin (Bsd) (Invitrogen Corp., Carlsbad, CA). hTNFR2/mFas-PA cells express a chimeric receptor derived from the extracellular and transmembrane domain of human TNFR2 fused to the intracellular domain of mouse Fas [19]. 293T cells and HeLaP4 cells were cultured in DMEM with 10% FBS and 1% antibiotic cocktail. HEp-2 cells are a human laryngeal squamous cell carcinoma cell line, and were cultured in RPMI-1640 medium supplemented with 10% FBS and 1% antibiotic cocktail.

2.2. Surface plasmon resonance (SPR) assay

The binding kinetics of wild-type TNF, mutant TNF-R1 and mutant TNF-R2 were analyzed by the SPR technique using a BIAcore 3000 (BIAcore[®], GE Healthcare, Buckinghamshire, UK). Human TNFR1 or human TNFR2 Fc chimeras (R&D systems, Minneapolis, MN) were diluted to 50 μ g/ml in 10 mM sodium acetate buffer (pH 4.5).

TNFRs were immobilized on a CM5 sensor chip, which resulted in an increase of 3000–3500 resonance units (RU). During the association phase, TNFs diluted in running buffer (HBS-EP) at 156.8, 52.3 or 17.4 nM were individually passed over the immobilized TNFRs at a flow rate of 20 μ l/min. During the dissociation phase, HBS-EP buffer was applied to the sensor chip at a flow rate of 20 μ l/min. The data were analyzed with BIAEVALUATION 3.0 software (BIAcore[®]) using a 1:1 binding model.

2.3. Cytotoxicity assays

HEp-2 cells were cultured in 96-well plates (4 \times 10⁴ cells/well) in a serial dilution of human TNF (Peprotech, Rocky Hill, NJ) or mutant TNFs with 100 μ g/ml cycloheximide. After incubation for 18 h, cell survival was determined using the methylene blue assay as described previously [17]. hTNFR2/mFas-PA were seeded onto 96-well plates at a density of 1.5 \times 10⁴ cells/well in culture medium. Serial dilutions of human TNF or paraformaldehyde-fixed M ϕ cells were prepared in DMEM containing 1 μ g/ml cycloheximide, and added to each well. After 48 h, cell viability was measured using the WST-assay kit (Nacalai Tesque) according to the manufacturer's instructions.

2.4. Construction of a self-inactivating (SIN) lentiviral vector

Vectors were constructed using standard cloning procedures. A DNA fragment encoding the precursor signal of human TNF was amplified by polymerase chain reaction (PCR) with the following primer pairs: forward primer-1 (5'-GAT TTC GAT ACG TAC GGA AGC TTC GTC GAC ATT AAT TAA GGA CAC CAT GAG CAC TGA AAG CAT GAT CCG GGA CGT GGA GCT GGC CGA GGA GG-3') containing a SalI site at the 5'-end, reverse primer-1 (5'-AGA GGC TGA GGA ACA AGC ACC GCC TGG AGC CCT GGG GCC CCC CTG TCT TCT TGG GGA GCG CCT CCT CGG CCA GCT CCA CGT CCC GGA TCA-3'), forward primer-2 (5'-GCT CCA GGC GGT GCT TGT TCC TCA GCC TCT TCT CCT TCC TGA TCG TGG CAG GCG CCA CCA CGC TCT TCT GCC TGC TGC ACT TTG GAG TGA-3'), and reverse primer-2 (5'-TGC CTG GGC CAG AGG GCG CGG CCG CGA GAT CTC TGG GGA ACT CTT CCC TCT GGG GGC CGA TCA CTC CAA AGT GCA GCA GGC AGA AGA GCG-3') containing BglII site at the 5'-end. The resulting amplified fragment was subcloned into the pY02 vector to generate pY02-preTNF. DNA fragments encoding non-cleavable wild-type human TNF (tm-wtTNF Δ 1–12) (Fig. 2a), TNFR1-selective mutant TNF (tm-mutTNF-R1 Δ 1–12), and TNFR2-selective mutant TNF (tm-mutTNF-R2 Δ 1–12) which were generated by deleting amino acids 1–12 in the N-terminal part of TNF, were amplified by PCR from wild-type TNF, mutant TNF-R1, and mutant TNF-R2 respectively with the following primer pairs: forward primer-3 (5'-AGT GAT CCG CCC CCA GAG GGA AGC TTA GAT CTC TCT CTA ATC AGC CCT CTG GCC CAG GCA GTA GCC CAT GTT GTA GCA AAC CCT CAAG-3') containing a BglII site at the 5'-end, and reverse primer-3 (5'-GGT TGG ATG TTC GTC CTC CGC GGC CGC CTA ACT AGT TCA CAG GGC AAT GAT CCC AAA GTA GAC CTG-3') containing a NotI site at the 5'-end. These fragments were cloned into the pY02-preTNF vector. Then, fragments of tm-wtTNF Δ 1–12, tm-mutTNF-R1 Δ 1–12, and tm-mutTNF-R2 Δ 1–12 were cloned between the SalI and NotI sites of the SIN vector construct, generating CSII-EF-tm-wtTNF-IRES-GFP, CSII-EF-tm-mutTNF-R1-IRES-GFP, and CSII-EF-tm-mutTNF-R2-IRES-GFP, respectively.

2.5. Preparation of lentiviral vectors

Lentiviral vectors were prepared as previously described [20,21]. In brief, 293T cells were transfected by the calcium phosphate method with three plasmids: packaging construct (pCAG-HIVgp), VSV-G and Rev expressing construct (pCMV-VSV-G-RSV-Rev) and

the SIN vector constructs (CSII-EF-tm-wtTNF-IRES-rhGFP, CSII-EF-tm-mutTNF-R1-IRES-rhGFP or CSII-EF-tm-mutTNF-R2-IRES-rhGFP) (Fig. 2b). Two days after transfection, the conditioned medium was collected and the virus was concentrated by ultracentrifugation at 50,000g for 2 h at 20 °C. The pelleted virus was re-suspended in Hank's balanced salt solution (GIBCO BRL, Paisley, UK). Vector titers were determined by measuring the infectivity of HeLaP4 cells with serial dilutions of vector stocks using flow cytometric analysis (FCM) for GFP-positive cells.

2.6. Creation of membrane-bound TNF expressing cells

To prepare tmTNF-expressing cells, DKO M ϕ (1×10^3 cells/well) cells were transfected with each lentiviral vector (tm-wtTNF, tm-mutTNF-R1 or tm-mutTNF-R2) at a multiplicity of infection (MOI) of 160 in 96-well plates. Infected cells were cultured until reaching 1×10^7 cells. IRES-driven GFP-positive cells were single-cell-sorted by FACS Vantage™ (BD Biosciences, Franklin Lakes, NJ), and cultured in conditioned medium from DKO M ϕ cells. After blocking Fc receptors with anti-mouse CD16/32 (eBioscience, San Diego, CA), the expression of tmTNF on monoclonal cell lines was detected by staining with Phycoerythrin-conjugated anti-human TNF antibody (clone MAb11, eBioscience) at $0.5 \mu\text{g}/5 \times 10^5$ cells for 30 min on ice. Subsequently, the cells were washed with 1% FBS/PBS and re-suspended in 500 μl of 4% paraformaldehyde. GFP or phycoerythrin fluorescence was analyzed using FCM by FACSCalibur™. Monoclonal cell lines stably expressing tmTNF or its mutants and GFP (tmTNF-expressing M ϕ , tm-wtTNF M ϕ , tm-mutTNF-R1 M ϕ , or tm-mutTNF-R2 M ϕ) were used for the following experiments.

2.7. Measurement of receptor binding activity by FCM

To detect the binding of soluble human TNFR1 (shTNFR1) or TNFR2 (shTNFR2) to tmTNF on M ϕ cell lines, shTNFR1- or shTNFR2-Fc chimera were labeled with R-phycoerythrin by Zenon™ Human IgG Labeling Kits (Invitrogen Corp.) according to the manufacturer's procedure. Briefly, 10 μl of shTNFR1- or shTNFR2-Fc chimera (250 $\mu\text{g}/\text{ml}$) (R&D systems) was incubated with 5 μl labeling reagent for 5 min at room temperature, and 5 μl blocking reagent was added to each reaction solution. After incubation for 5 min at room temperature, 4 μl each reaction solution was added to 5×10^5 cells/tube which were pretreated with mouse Fc block. After incubation for 30 min on ice, the cells were washed with 1% FBS/PBS, and then suspended in 500 μl of 0.4% paraformaldehyde.

3. Results and discussion

An understanding of the bioactivity of tmTNF is key to a better understanding of the overall function of TNF and TNF receptors. The relative contribution of signaling by tmTNF through the TNFR1 and TNFR2 receptors is unclear, as it is difficult to monitor the specific activation of these two receptors in response to tmTNF. To address this problem, we established macrophage cell lines expressing TNFR-selective mutant TNFs (tmTNF-R1 or tmTNF-R2) on the cell surface.

First, to assess the receptor selectivity of soluble mutTNF-R1 or R2 (sol-mutTNF-R1 or R2), which we previously created using a phage display system [18], we measured human TNFR1-mediated bioactivities of sol-mutTNFs on HEP-2 cells and human TNFR2-mediated bioactivities on hTNFR2/mFas-PA cells (Fig. 1a and Table 1). The binding affinity and kinetic parameters of these mutant TNFs for each TNF receptor were also measured using a Surface plasmon resonance assay (Fig. 1b and Table 1). We observed that

both the bioactivity and binding affinity of sol-mutTNF-R1 for hTNFR1 were equivalent to those of sol-wtTNF, whereas the activity and affinity of sol-mut-TNF-R1 for hTNFR2 were decreased to less than 0.2% and 8%, respectively, of the values observed with sol-wtTNF. Although the bioactivity of sol-mutTNF-R2 mediated via hTNFR2 was only 16% of that of sol-wtTNF, the binding affinity of sol-mutTNF-R2 for human TNFR2 was about 1.5 times higher than that of sol-wtTNF. The bioactivity and binding affinity of sol-mutTNF-R2 for hTNFR1 were decreased to less than 0.1% and 3%, respectively, of the corresponding values for sol-wtTNF. Interestingly, the kinetic parameters, k_{on} and k_{off} , of the sol-mutTNFs for the TNF receptors tended to be higher than those of sol-wtTNF, indicating rapid association/dissociation interaction. From these data, we confirmed a significant TNFR-selectivity of sol-mutTNF-R1 and sol-mutTNF-R2. Therefore, we attempted to create the corresponding TNFR-selective tmTNFs using these sol-mutTNFs.

To express only tmTNF on the cell surface, the recombinant genes corresponding to each sol-TNF mutant, each encoding a protein with an additional twelve amino acid deletion from the N-terminus, were subcloned into lentiviral vectors (Fig. 2a and b). The resulting recombinant lentiviral vectors were transduced into TNFR1^{-/-}R2^{-/-} macrophages (DKO M ϕ). As previously reported, the deletion of the first 12 amino acids from the N-terminus of TNF, including the entire TACE cleavage site, leads to the expression of only the tmTNF form, and not the soluble form [15,22]. Since the SIN vector also comprises a GFP expression cassette, GFP expression was visible in all three cell lines: wtTNF-expressing DKO M ϕ (tm-wtTNF M ϕ), mutTNF-R1 expressing DKO M ϕ (tm-mutTNF-R1 M ϕ), and mutTNF-R2 expressing DKO M ϕ (tm-mutTNF-R2 M ϕ) (Fig. 2c). We next verified the expression of TNF on single sorted cells using FCM analysis. We observed significant expression of TNF on tm-wtTNF M ϕ (Fig. 3a). The mean fluorescence intensity (MFI) of tm-mutTNF-R1 M ϕ and tm-mutTNF-R2 M ϕ was lower than that of tm-wtTNF M ϕ (Fig. 3b). Since the expression level of GFP on tm-mutTNF-R1 M ϕ and tm-mutTNF-R2 M ϕ was lower than that on tm-wtTNF M ϕ (Fig. 2c), the expression level of TNF on these cells might also be lower than that on tm-wtTNF M ϕ .

Next, the affinity of each cell-surface expressed tmTNF for soluble TNF receptors was measured by FCM analysis (Fig. 4a), and receptor selectivity was estimated (Fig. 4b and c). We observed that both soluble TNFR1 and TNFR2 Fc chimeras bound to tm-wtTNF M ϕ , although TNFR2 bound to tm-wtTNF M ϕ with an affinity approximately twofold stronger than that of TNFR1 (Fig. 4b). Although the affinity of tm-mutTNF-R1 M ϕ for TNFR1 was 50% that of tm-wtTNF M ϕ , the affinity of tm-mutTNF-R1 M ϕ for TNFR2 was greatly decreased and the ratio of selectivity of tm-mutTNF-R1 M ϕ for TNFR1 over TNFR2 (R1/R2 of MFI) was approximately three times that of tm-wtTNF M ϕ (Fig. 4b and c). Therefore, the expression of mutTNF-R1 on the cell surface as the tmTNF form demonstrates TNFR1 selectivity, as does its soluble form. On the other hand, the affinity of TNFR1 and TNFR2 for tm-mutTNF-R2 M ϕ was weaker than their affinity for tm-wtTNF M ϕ (Fig. 4a and b). Additionally, the ratio of selectivity of tm-mutTNF-R2 M ϕ for TNFR1 over TNFR2 was similar to that of tm-wtTNF M ϕ , indicating little selectivity for TNFR2 in contrast to what was observed for sol-mutTNF-R2 (Fig. 4c). We next evaluated the bioactivity of these tmTNFs via hTNFR2, by assessing the cytotoxicity of these tmTNFs on hTNFR2/mFas-PA cells, which express the hTNFR2/mFas chimeric receptor (Fig. 5). As previously reported, a cytotoxicity assay using hTNFR2/mFas-PA cells is a simple and highly sensitive assay system for determining TNFR2-mediated activity. DKO M ϕ expressing each type of tmTNF (effector cell) were fixed with paraformaldehyde, and co-cultured with hTNFR2/mFas-PA cells (target cell). The viability of the target cells decreased significantly and in a dose-dependent manner

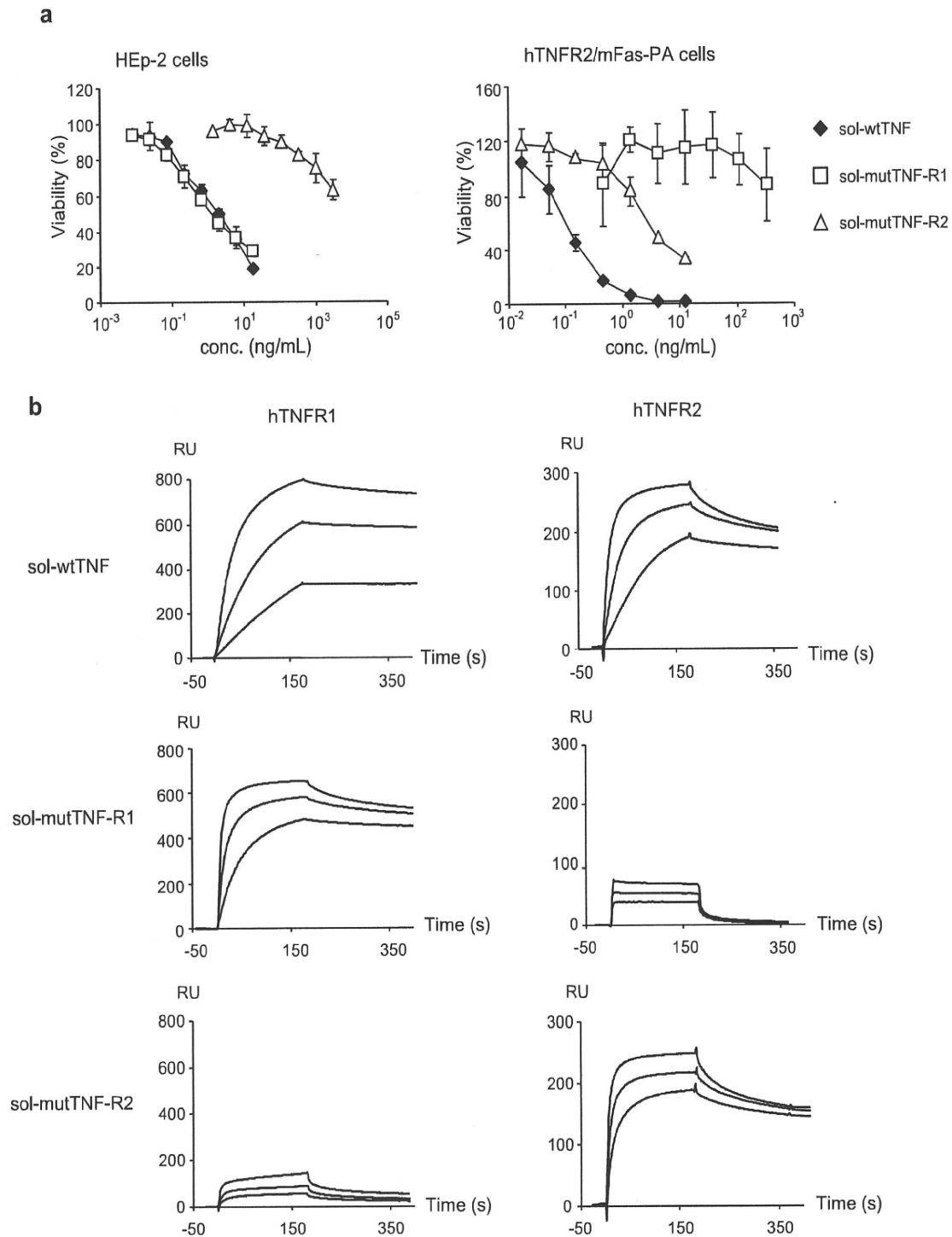


Fig. 1. Bioactivity and binding of sol-wtTNF, sol-mutTNF-R1, and sol-mutTNF-R2 to TNFRs. (a) HEP-2 cells or hTNFR2/Fas-PA cells were used for measuring TNFR1-mediated or TNFR2-mediated bioactivity respectively. HEP-2 cells were cultured in serial dilutions of sol-wtTNF, sol-mutTNF-R1, and sol-mutTNF-R2 with 100 μ g/ml cycloheximide for 18 h. hTNFR2/Fas-PA cells were also cultured in serial dilutions of sol-TNFs with 1 μ g/ml cycloheximide for 48 h. Cell viability was determined using the methylene blue assay for HEP-2 cells, and the WST-8 assay for hTNFR2/Fas-PA cells. (b) The binding kinetics of sol-TNFs to immobilized TNFRs were analyzed using the surface plasmon resonance (SPR) technique. TNFRs were immobilized to a sensor chip CM5, which resulted in an increase of 3000–3500 resonance units (RU). The amount of protein bound to the surface was recorded in RU. Duplicate injections of 156.8, 52.3, or 17.4 nM sol-TNFs were passed over the immobilized TNFRs at a flow rate of 20 μ l/min. The sensorgrams shown were normalized by subtracting the control surface sensorgram.

when exposed to an increasing $E(\text{effector})/T(\text{target})$ cell ratio of tm-wtTNF $M\phi$ compared to exposure to the control DKO $M\phi$. These results suggest that tmTNF induced death of these cells

in a dose-dependent manner via signaling through the TNFR2/mFas chimera expressed on the target cell surface. The bioactivity of tm-mutTNF-R1 $M\phi$ was lower than that of tm-wtTNF $M\phi$ in

Table 1
Amino acid sequence, bioactivity, and kinetic parameters of mutTNFs.

Human TNFs	Amino acids sequence						Bioactivity EC50 (nM)		Binding property					
									TNFR1			TNFR2		
	29	31	32	145	146	147	HEp-2	hTNFR2/ mFas-PA	k_{on} ($M^{-1} S^{-1}$) ^a	k_{off} (s^{-1}) ^b	k_d (nM) ^c	k_{on} ($M^{-1} S^{-1}$) ^a	k_{off} (S^{-1}) ^b	k_d (nM) ^c
sol-wtTNF	L	R	R	A	E	S	1.9 (100%)	0.5 (100%)	2.1×10^5	1.4×10^{-4}	0.68 (100%)	1.1×10^6	7.8×10^{-4}	0.70 (100%)
sol-mutTNF-R1	K	A	G	A	S	T	1.5 (128%)	>300 (<0.2%)	6.5×10^5	4.7×10^{-4}	0.73 (93%)	5.8×10^6	522.0×10^{-4}	9.0 (8%)
sol-mutTNF-R2	L	R	R	R	E	T	>3000 (<0.1%)	3.1 (16%)	1.8×10^5	36.1×10^{-4}	20.2 (3%)	3.1×10^6	15.4×10^{-4}	0.49 (144%)

Kinetic parameters for each TNF were calculated by from the respective sensorgrams by BIA evaluation 3.0 software. Value in parenthesis shows the relative bioactivity or relative binding affinity (%).

^a k_{on} is association kinetic constant.

^b k_{off} is dissociation kinetic constant.

^c k_d (equilibrium dissociation constant) denotes binding affinity.

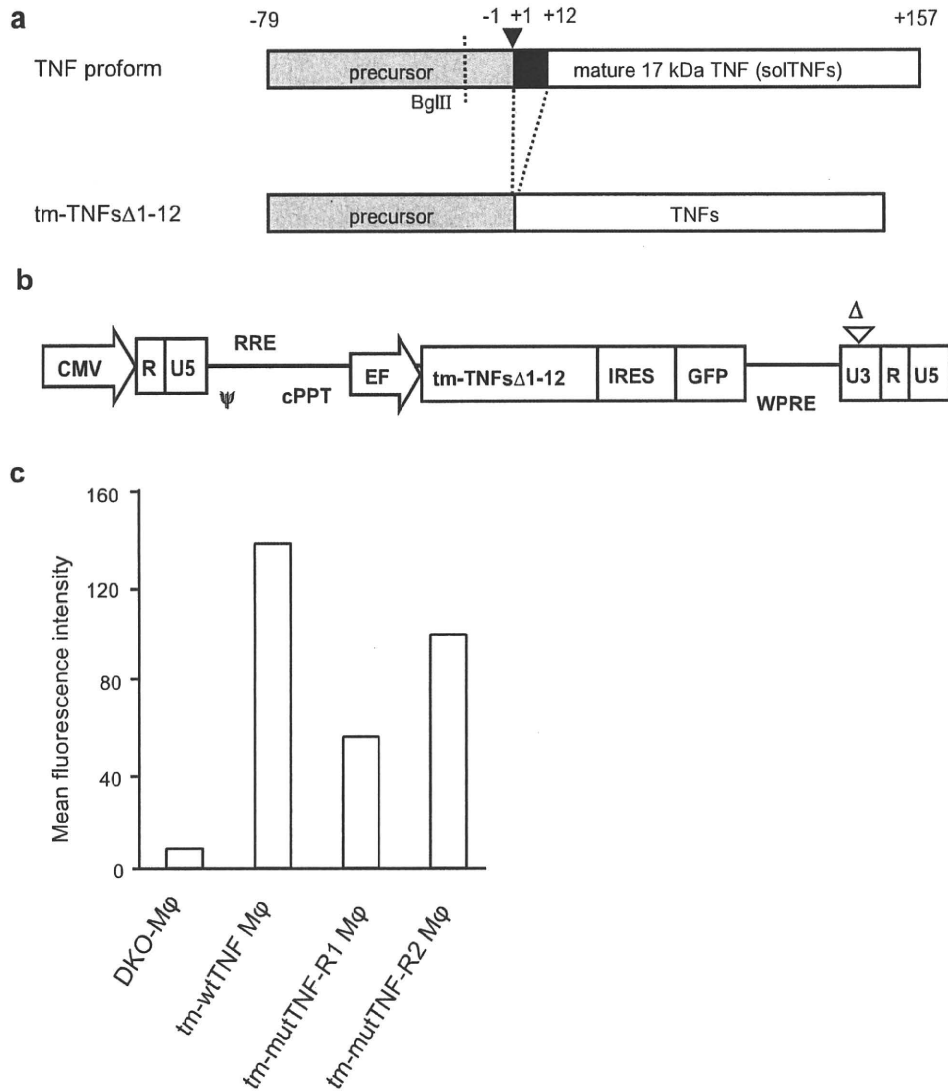


Fig. 2. Schematic representation of the tmTNF forms and the construction of the lentiviral vector. (a) Schematic representation of non-cleavable human TNFs (tm-TNFsΔ1–12). An inverted filled triangle shows the cleavage site. Closed bar, amino acids 1–12, indicates the deleted region. (b) Schematic representation of self-inactivating (SIN) LV plasmid (CSII-EF-tm-TNFsΔ1–12-IRES-GFP). CMV: cytomegalovirus promoter, ψ: packaging signal, RRE: rev responsive element, cPPT: central polyurine tract, IRES: Encephalomyocarditis virus internal ribosomal entry site, Bsd: Blasticidin, WPRE: woodchuck hepatitis virus posttranscriptional regulatory element. Δ: deletion of 133 bp in the U3 region of the 3' long terminal repeat. (c) Expression of GFP on each cell was analyzed by FCM, and the mean fluorescence intensity of each cell is shown.

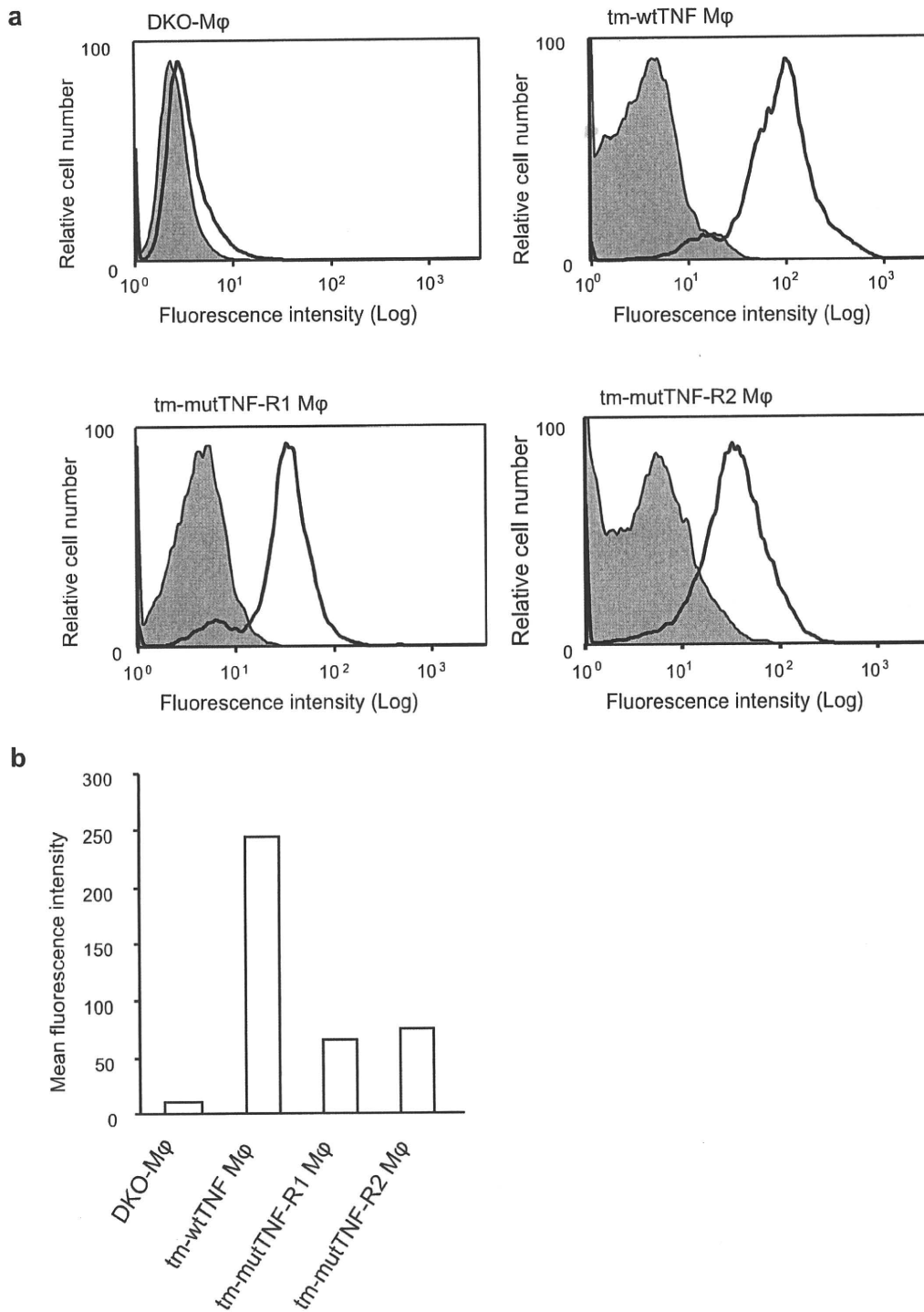


Fig. 3. The expression of TNF as the transmembrane form on tm-TNFs Mφ. (a) Expression of TNF on each cell was analyzed by FCM using PE-conjugated anti-hTNF monoclonal antibody (open histograms) or PE-conjugated isotype control antibody (shaded histograms). (b) The mean fluorescence intensity of each cell is shown.

this assay, which correlates with the results observed when studying its soluble form in Table 1. Interestingly, tm-mutTNF-R2 Mφ was more cytotoxic than tm-wtTNF Mφ, whereas the cytotoxicity of sol-mutTNF-R2 was only 16% of that of sol-wtTNF in this assay.

In this study, we have established the selectivity of tm-mutTNF-R1 Mφ for binding to TNFR1, although we need to measure the precise expression level of TNF in each cell. In addition, FCM analysis suggested that tm-mutTNF-R2 Mφ have a lower affinity for both TNFRs than do tm-wtTNF Mφ, and that they exhibit little selectivity

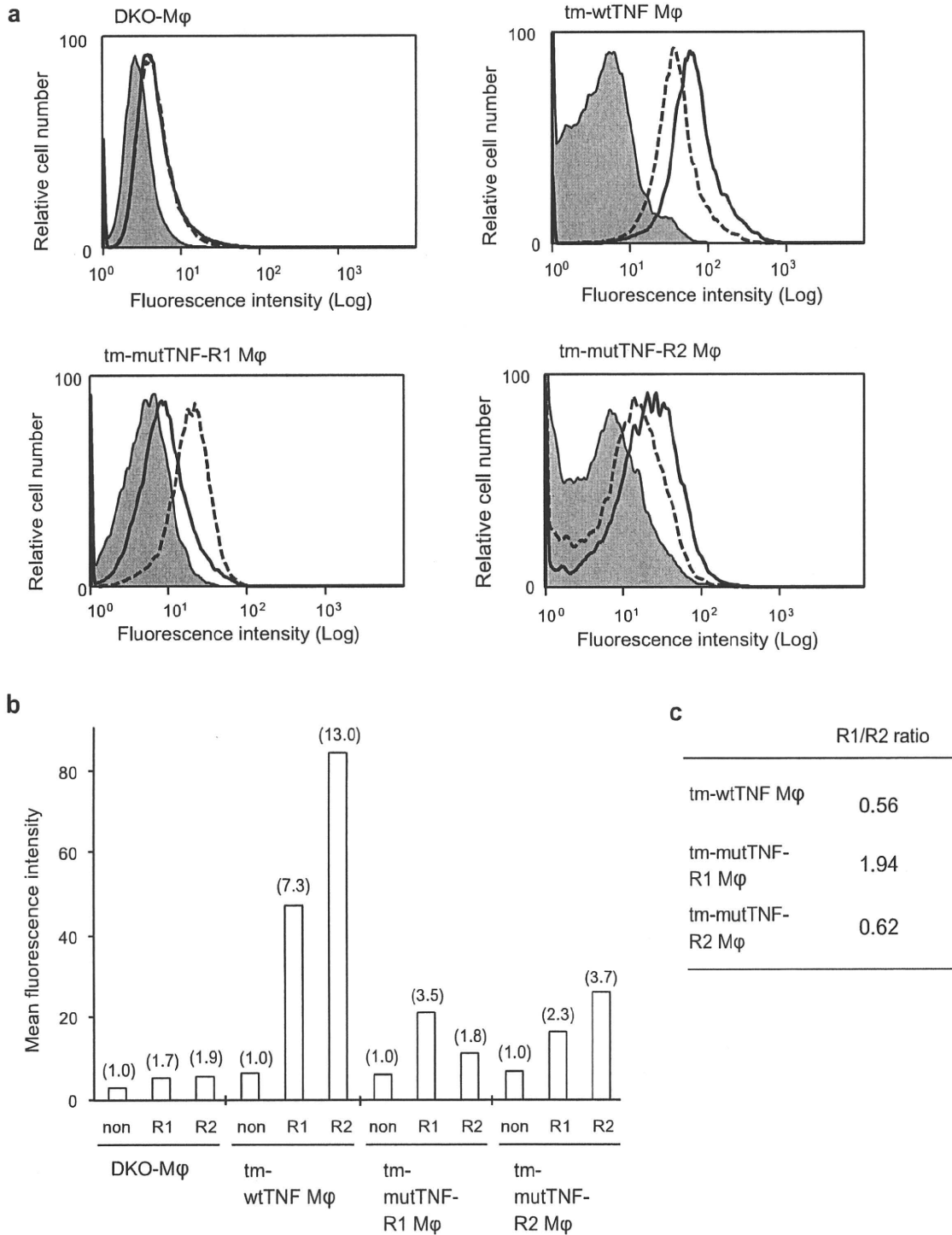


Fig. 4. The affinity of tm-TNFs Mφ for soluble TNF-receptors. (a) The binding of each tmTNF to solTNFR1 (dashed lines) or solTNFR2 (solid lines) was analyzed by FCM analysis. DKO Mφ, tm-wtTNF Mφ, tm-mutTNF-R1 Mφ, and tm-mutTNF-R2 Mφ were stained with solTNFR1- or solTNFR2-Fc chimera that was labeled with PE-conjugated Fab fragment of anti-human Fc antibody. Shaded histograms show non-stained cells. (b) Mean fluorescence intensity of each cells is shown. (c) Values in parenthesis indicate the relative intensity against non-treated cells in each cell line.

for TNFR2. In this report, we established macrophage cell lines expressing only tmTNF, and not solTNF, owing to the deletion of the first 12 amino acids ($\Delta 1-12$) of each TNF mutant. Although

most studies have made use of the $\Delta 1-12$ TNF mutation for the investigation of tmTNF activity, the bioactivity of the resulting non-cleavable tmTNF is reported to be reduced compared to

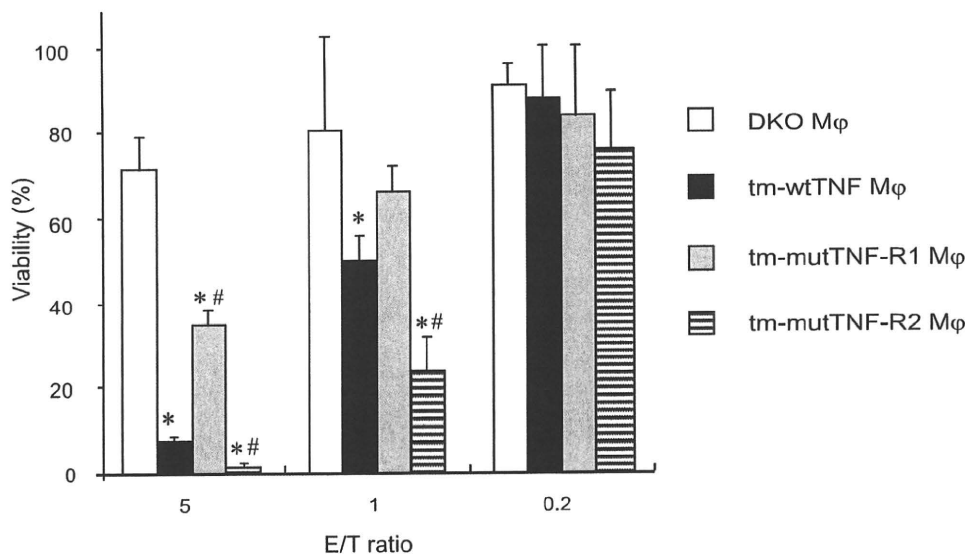


Fig. 5. tm-mutTNF-R2 Mφ induced death of hTNFR2/mFas-PA cells. hTNFR2/mFas-PA cells were co-incubated with paraformaldehyde-fixed DKO Mφ (open bars), tm-wtTNF Mφ (filled bars), tm-mutTNF-R1 Mφ (shaded bars), or tm-mutTNF-R2 Mφ (stiped bars) at an effector/target (E/T) ratio of 5:1, 1:1, or 0.2:1 in the presence of cycloheximide (1 μg/ml). After 48 h, cell viability was measured by the WST-8 Assay. Data were expressed as mean values ± SD of triplicate measurements and analyzed by one-way ANOVA (Dunnett's test). **p* < 0.05: compared to DKO Mφ, #*p* < 0.05: compared to tm-wtTNF Mφ.

wild-type tmTNF, whereas a tmTNF mutant containing a Δ1–9 K11E mutation exhibited normal cell-surface expression and a bioactivity similar to the wild-type [22]. Therefore, use of this latter deletion backbone may allow greater TNFR-selectivity in Mφ engineered to express tm-mutTNF-R2, and may generate superior TNFR-selective tmTNF-expressing cells.

As described earlier, tmTNF and solTNF have distinct roles or functions in normal and pathological conditions [8]. Furthermore, it is also believed that TNFR2 can only be fully activated by tmTNF [23]. Although the mechanisms underlying these effects are poorly understood, the half lives of the individual ligand/receptor complexes may contribute to the differential activity of tmTNF and solTNF [23]. Krippner-Heidenreich et al. reported that the dissociation rate constant of the cell surface binding of tmTNF to TNFR2 is much lower than that of the binding of solTNF to the same receptor, indicating that tmTNF dissociates much less readily from TNFR2 [24]. Thus, the bioactivity imparted by the interaction of the ligand/receptor pair is dependent upon various binding parameters (binding affinity, association or dissociation rate constant). We have shown here that tm-mutTNF-R2 Mφ exhibit greater cytotoxicity on hTNFR2/mFas-PA cells than do tm-wtTNF Mφ, whereas the cytotoxicity of sol-mutTNF-R2 was lower than that of sol-wtTNF. We assume that the dissociation rate constant of the binding of mutTNF-R2 to immobilized TNFR2 or TNFR2 on the cell surface might be reduced to a level similar to that of tm-wtTNF Mφ upon conversion of the soluble form to the transmembrane form. As such, the threefold higher association rate constant of the interaction of TNFR2 with sol-mutTNF-R2 than that of TNFR2 with sol-wtTNF (Table 1) might explain the strong bioactivity on hTNFR2/mFas-PA cells.

The affinity between a ligand and its receptor is determined by an equilibrium between the rates of association and dissociation, and is determined inherently. Therefore, expression of sol-mut-TNFs with selectivity for each TNFR as the corresponding tmTNF forms on the cell surface, may alter the selectivity for the TNFRs. We plan to carry out more detailed analyses of the variant tmTNFs, such as measurement of their expression, their precise affinity for TNFR1 or R2, and their activity mediated through binding and signaling through TNFR1. Eventually, these tmTNFs, tm-mutTNF-R1 and R2 Mφ may prove useful for functional analysis or signal analysis of TNF receptors.

Acknowledgments

This study was supported in part by some Grants-in-Aid for Scientific Research from the Ministry of Education, Culture, Sports, Science and Technology of Japan, and in part by some Grants-in-Aid for Scientific Research from Japan Society for the Promotion of Science (JSPS). And this study was also supported in part by some Health Labour Sciences Research Grants from the Ministry of Health, Labor and Welfare of Japan, and in part by Health Sciences Research Grants for Research on Publicly Essential Drugs and Medical Devices from the Japan Health Sciences Foundation, in part by The Nagai Foundation Tokyo.

References

- [1] Aggarwal BB. Signalling pathways of the TNF superfamily: a double-edged sword. *Nat Rev Immunol* 2003;3:745–56.
- [2] Beutler B. Autoimmunity and apoptosis: the Crohn's connection. *Immunity* 2001;15:5–14.
- [3] Feldmann M, Maini RN. Anti-TNF alpha therapy of rheumatoid arthritis: what have we learned? *Annu Rev Immunol* 2001;19:163–96.
- [4] Feldmann M. Development of anti-TNF therapy for rheumatoid arthritis. *Nat Rev Immunol* 2002;2:364–71.
- [5] Kriegler M, Perez C, DeFay K, Albert I, Lu SD. A novel form of TNF/cachectin is a cell surface cytotoxic transmembrane protein: ramifications for the complex physiology of TNF. *Cell* 1988;53:45–53.
- [6] Tang P, Hung MC, Klostergaard J. Human pro-tumor necrosis factor is a homotrimer. *Biochemistry* 1996;35:8216–25.
- [7] Black RA, Rauch CT, Kozlosky CJ, Peschon JJ, Slack JL, Wolfson MF, et al. A metalloproteinase disintegrin that releases tumour-necrosis factor- α from cells. *Nature* 1997;385:729–33.
- [8] Ruuls SR, Hoek RM, Ngo VN, McNeil T, Lucian LA, Janatpour MJ, et al. Membrane-bound TNF supports secondary lymphoid organ structure but is subservient to secreted TNF in driving autoimmune inflammation. *Immunity* 2001;15:533–43.
- [9] Mueller C, Corazza N, Trachsel-Loseth S, Eugster HP, Buhler-Jungo M, Brunner T, et al. Noncleavable transmembrane mouse tumor necrosis factor- α (TNF α) mediates effects distinct from those of wild-type TNF α in vitro and in vivo. *J Biol Chem* 1999;274:38112–8.
- [10] Olleros ML, Guler R, Vesin D, Parapanov R, Marchal G, Martinez-Soria E, et al. Contribution of transmembrane tumor necrosis factor to host defense against *Mycobacterium bovis* bacillus Calmette-guerin and *Mycobacterium tuberculosis* infections. *Am J Pathol* 2005;166:1109–20.
- [11] Saunders BM, Tran S, Ruuls S, Sedgwick JD, Briscoe H, Britton WJ. Transmembrane TNF is sufficient to initiate cell migration and granuloma formation and provide acute, but not long-term, control of *Mycobacterium tuberculosis* infection. *J Immunol* 2005;174:4852–9.

- [12] Torres D, Janot L, Quesniaux VF, Grivennikov SI, Maillet I, Sedgwick JD. Membrane tumor necrosis factor confers partial protection to *Listeria* infection. *Am J Pathol* 2005;167:1677–87.
- [13] Aggarwal BB, Eessalu TE, Hass PE. Characterization of receptors for human tumour necrosis factor and their regulation by gamma-interferon. *Nature* 1985;318:665–7.
- [14] Micheau O, Tschopp J. Induction of TNF receptor I-mediated apoptosis via two sequential signaling complexes. *Cell* 2003;114:181–90.
- [15] Perez C, Albert I, DeFay K, Zachariades N, Gooding L, Kriegler M. A nonsecretable cell surface mutant of tumor necrosis factor (TNF) kills by cell-to-cell contact. *Cell* 1990;63:251–8.
- [16] Bryde S, Grunwald I, Hammer A, Krippner-Heidenreich A, Schiestel T, Brunner H, et al. Tumor necrosis factor (TNF)-functionalized nanostructured particles for the stimulation of membrane TNF-specific cell responses. *Bioconjug Chem* 2005;16:1459–67.
- [17] Shibata H, Yoshioka Y, Ohkawa A, Minowa K, Mukai Y, Abe Y, et al. Creation and X-ray structure analysis of the tumor necrosis factor receptor-1-selective mutant of a tumor necrosis factor-alpha antagonist. *J Biol Chem* 2008;283:998–1007.
- [18] Mukai Y, Shibata H, Nakamura T, Yoshioka Y, Abe Y, Nomura T, et al. Structure-function relationship of tumor necrosis factor (TNF) and its receptor interaction based on 3D structural analysis of a fully active TNFR1-selective TNF mutant. *J Mol Biol* 2009;385:1221–9.
- [19] Abe Y, Yoshikawa T, Kamada H, Shibata H, Nomura T, Minowa K, et al. Simple and highly sensitive assay system for TNFR2-mediated soluble- and transmembrane-TNF activity. *J Immunol Methods* 2008;335:71–8.
- [20] Katayama K, Wada K, Miyoshi H, Ohashi K, Tachibana M, Furuki R, et al. RNA interfering approach for clarifying the PPARgamma pathway using lentiviral vector expressing short hairpin RNA. *FEBS Lett* 2004;560:178–82.
- [21] Miyoshi H, Smith KA, Mosier DE, Verma IM, Torbett BE. Transduction of human CD34+ cells that mediate long-term engraftment of NOD/SCID mice by HIV vectors. *Science* 1999;283:682–6.
- [22] Decoster E, Vanhaesebroeck B, Vandenamee P, Grooten J, Fiers W. Generation and biological characterization of membrane-bound, uncleavable murine tumor necrosis factor. *J Biol Chem* 1995;270:18473–8.
- [23] Grell M, Douni E, Wajant H, Lohden M, Clauss M, Maxeiner B, et al. The transmembrane form of tumor necrosis factor is the prime activating ligand of the 80 kDa tumor necrosis factor receptor. *Cell* 1995;83:793–802.
- [24] Krippner-Heidenreich A, Tubing F, Bryde S, Willi S, Zimmermann G, Scheurich P. Control of receptor-induced signaling complex formation by the kinetics of ligand/receptor interaction. *J Biol Chem* 2002;277:44155–63.

National Institute of Biomedical Innovation (NiBio)¹; Graduate School of Pharmaceutical Sciences², Osaka University; The Center for Advanced Medical Engineering and Informatics³, Osaka University, Osaka, Japan

Creation of an improved mutant TNF with TNFR1-selectivity and antagonistic activity by phage display technology

T. NOMURA^{1,2*}, Y. ABE^{1*}, H. KAMADA^{1,3}, M. INOUE¹, T. KAWARA^{1,2}, S. ARITA^{1,2}, T. FURUYA^{1,2}, K. MINOWA¹, Y. YOSHIOKA^{2,3}, H. SHIBATA¹, H. KAYAMURO^{1,2}, T. YAMASHITA^{1,2}, K. NAGANO¹, T. YOSHIKAWA^{1,2}, Y. MUKAI², S. NAKAGAWA^{2,3}, S. TSUNODA^{1,2,3}, Y. TSUTSUMI^{1,2,3}

Received August 7, 2009, accepted August 14, 2009

Shin-ichi Tsunoda, Ph.D., Laboratory of Pharmaceutical Proteomics, National Institute of Biomedical Innovation, 7-6-8 Saito-Asagi, Ibaraki, Osaka 567-0085, Japan
tsunoda@nibio.go.jp

*These authors contributed equally to the work.

Pharmazie 65: 93–96 (2010)

doi: 10.1691/ph.2010.9265

Tumor necrosis factor- α (TNF), which binds two types of TNF receptors (TNFR1 and TNFR2), regulates the onset and exacerbation of autoimmune diseases such as rheumatoid arthritis and Crohn's disease. In particular, TNFR1-mediated signals are predominantly related to the induction of inflammatory responses. We have previously generated a TNFR1-selective antagonistic TNF-mutant (mutTNF) and shown that mutTNF efficiently inhibits TNFR1-mediated bioactivity *in vitro* and attenuates inflammatory conditions *in vivo*. In this study, we aimed to improve the TNFR1-selectivity of mutTNF. This was achieved by constructing a phage library displaying mutTNF-based variants, in which the amino acid residues at the predicted receptor binding sites were substituted to other amino acids. From this mutant TNF library, 20 candidate TNFR1-selective antagonists were isolated. Like mutTNF, all 20 candidates were found to have an inhibitory effect on TNFR1-mediated bioactivity. However, one of the mutants, N7, displayed significantly more than 40-fold greater TNFR1-selectivity than mutTNF. Therefore, N7 could be a promising anti-autoimmune agent that does not interfere with TNFR2-mediated signaling pathways.

1. Introduction

The severity and progression of inflammatory diseases, such as rheumatoid arthritis, Crohn's disease and ulcerative colitis, can be correlated with the serum level of tumor necrosis factor- α (TNF). Thus, TNF blockades such as anti-TNF antibodies and soluble TNFRs, which neutralize the activity of TNF, have been used to treat various autoimmune diseases in clinical practice. However, TNF blockades inhibit both TNFR1 and TNFR2 signaling. Thus, treatment with these drugs can lead to an increased risk of infection (Gomez-Reino et al. 2003; Lubel et al. 2007) and lymphoma development (Brown et al. 2002). TNF has been reported to induce inflammatory response predominantly through TNFR1 (Mori et al. 1996), whereas activation of the immune response is initiated *via* TNFR2 (Kim et al. 2006; Kim and Teh 2001; Grell et al. 1998). Therefore, blocking TNFR1-signaling, but not TNFR2-signaling, is a promising strategy for the safe and effective treatment of inflammatory diseases, which overcomes the risk of infection associated with the use of non-specific TNF blockades (Kollias and Kontoyiannis 2002). In our previous studies, we used the phage display technique (Imai et al. 2008; Nagano et al. 2009; Nomura et al. 2007) to generate a TNFR1-selective antagonistic mutant TNF (mutTNF) that blocks TNFR1-mediated signals but not those of TNFR2 (Shibata et al. 2008b). Moreover, mutTNF showed superior therapeutic effects using an inflammatory disease mouse model (Shibata et al. 2008a). Thus, a drug for autoimmune diseases that selectively targets TNFR1 is anticipated to display

higher efficacy and safety compared to existing treatments. In this study, we have attempted to isolate TNFR1-selective antagonists with higher TNFR1-selectivity than previous mutTNF by constructing a modified phage library displaying mutTNF-based variants.

2. Investigations, results and discussion

Here, we attempted to improve the TNFR1-selectivity of mutTNF using a phage display technique. Firstly, we constructed a phage library of TNF mutant using mutTNF as template. We designed a randomized library of mutTNF to replace the six amino acid residues (aa 29, 31, 32, 145–147) in the predicted receptor binding site. As a result of the 2-step PCR, we confirmed that the mutTNF mutant library consisted of 4×10^7 independent recombinant clones (*data not shown*). To enrich for TNFR1-selective antagonists, the phage library was subjected to two rounds of panning against TNFR1 on a Biacore biosensor chip. After the second panning, supernatants of single clone of *E. coli* TG1 including phagemid were randomly collected and subjected to screening by bioassay and ELISA to evaluate their bioactivity and affinity against each TNF receptor, respectively (*data not shown*). Consequently, twenty candidates of TNFR1-selective mutants with antagonistic activity were isolated (Table).

Next, we determined the detailed biological properties of each candidate. Positive clones were engineered for expression in

Table: Amino acid sequences and biological properties of TNFR1-selective antagonist candidates

TNF	Amino acid sequence						Relative affinity (% K_d) ^{a)}			Bioactivity via TNFR1	
	29	31	32	145	146	147	TNFR1	TNFR2	TNFR1 ^{b)} /TNCR2	Agonistic ^{c)} activity	Antagonist ^{d)} activity
mutTNF	L	R	R	A	E	S	100.0	100.0	1.0	-	+
N1	S	-	W	R	-	-	550.0	21.6	25.5	+	-
N2	S	-	W	-	-	-	200.0	N.D.	N.D.	+	-
N3	S	-	W	R	D	-	550.0	44.8	12.3	-	±
N4	S	-	W	-	D	-	183.3	19.1	9.6	±	-
N5	S	-	W	-	S	E	275.0	25.8	10.7	±	-
N6	A	D	T	-	-	-	200.0	21.6	9.3	±	-
N7	S	N	D	D	A	-	104.7	2.5	41.9	-	+
N8	R	I	A	D	-	-	169.2	26.7	6.3	+	-
N9	H	H	-	-	N	G	169.2	33.0	5.1	+	-
N10	T	N	N	-	-	-	314.3	28.6	11.0	±	-
N11	T	N	N	S	-	-	275.0	18.3	15.0	±	-
N12	F	S	T	-	-	-	440.0	58.0	7.6	+	-
N13	F	S	T	-	S	E	440.0	73.9	6.0	+	-
N14	R	W	Y	T	N	T	314.3	19.2	16.4	+	-
N15	F	K	T	N	A	T	275.0	24.1	11.4	±	-
N16	M	L	T	N	S	T	367.0	7.7	47.7	+	-
N17	Y	L	A	T	H	T	137.5	1.6	86.0	±	-
N18	Y	L	A	T	H	-	110.0	4.7	23.4	±	-
N19	V	Q	Y	N	N	-	367.0	N.D.	N.D.	±	-
N20	F	S	T	P	Q	R	244.4	N.D.	N.D.	±	-

Conserved residues compared with mutTNF are indicated by an em dash (-) The affinity values are shown as relative values (% mutTNF). N.D.: not detected

^{a)} Affinity for immobilized TNFR1 and TNFR2 was assessed by SPR using BIAcore3000. The dissociation constant (K_d) of TNF mutants were calculated from their sensorgrams by BIAEVALUATION 4.0 software

^{b)} TNFR1-selectivity was defined as relative affinity [TNFE1]/ relative affinity [TNFR2] for mutTNF

^{c)} TNFR1-mediated agonistic activity was measured, using a HEp-2 cell cytotoxicity assay. The intensity in agonistic activity was evaluated as the following. Cell viability at 10^4 ng/ml each mutant. 0–25% (of non treatment); (+), 25–50%; (±), 50–100%; (-)

^{d)} TNFR1-mediated antagonistic activity of mutant TNFs on wtTNF induced cytotoxicity in HEp-2 cells was measured. The intensity in antagonistic activity was evaluated as the following. Cell viability at 10^5 ng/ml each mutant in present of 5 ng/ml wtTNF. 0–25% (of non treatment); (-), 25–50%; (±), 50–100%; (+)

E. coli BL21λDE3 and each recombinant protein was purified as described previously (Yamamoto 2003). As anticipated, gel electrophoresis confirmed the mutant TNF proteins to have a molecular weight of 17 kDa. Moreover, gel filtration chromatography established that each mutant forms a homotrimeric complex in solution, as is the case for wild-type TNF (wtTNF) (data not shown). To analyze the binding properties of these TNFR1-selective TNF candidates, their dissociation constants (K_d) for TNFR1 and TNFR2 were measured using a surface

plasmon resonance (SPR) analyzer. Our previous SPR analysis showed that although mutTNF has an almost identical affinity to TNFR1 as to wtTNF, it displays more than 17,000-fold greater selectivity for TNFR1. As shown in the Table, all the candidates exhibited higher affinity for TNFR1 than mutTNF. Furthermore, clones N1, N7, N16, N17 and N18 showed more than 20-fold higher TNFR1-binding selectivity compared to mutTNF. To examine the bioactivity of all candidates via TNFR1, we subsequently performed a cytotoxicity assay using

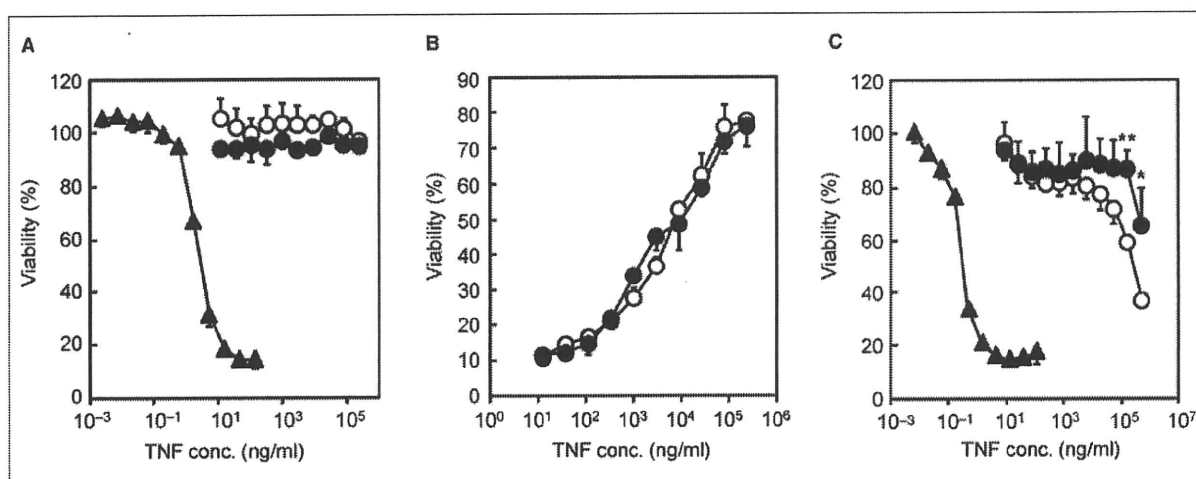


Fig. 3: Bioactivities and antagonistic activities of N7. (A) To determine the TNFR1-mediated bioactivities, several dilutions of wtTNF (closed triangle), mutTNF (open circle) and N7 (closed circle) were added to L-M cells and incubated for 4 h at 37 °C. (B) Indicated dilutions of mutTNF (open circle) and N7 (closed circle) and constant of wtTNF (5 ng/ml) were mixed and added to L-M cells and incubated for 4 h at 37 °C. TNFR1-mediated antagonistic activity was assessed as described in the Experimental section. (C) To determine the TNFR2-mediated bioactivities, diluted wtTNF (closed triangle), mutTNF (open circle) and N7 (closed circle) were added to hTNFR2/mFas-preadipocyte cells and incubated for 48 h at 37 °C. After incubation, cell viability was measured using the methylene blue assay. Data represent the mean \pm S.D. and were analyzed by Student's t-test (* $p < 0,05$, ** $p < 0,01$ vs mutTNF)

HEp-2 cells (Table). As anticipated, mutTNF was unable to activate TNFR1. Likewise clones N3 and N7 do not activate TNFR1 signaling, even when tested at high concentrations. The TNFR1-mediated antagonistic assay demonstrated that N7 showed the highest activity of all the TNFR1-selective antagonist candidates. The Figure show details of bioactivities and antagonistic activities of N7. The TNFR1-mediated agonistic activity using L-M cells showed that wtTNF displays TNFR1-mediated agonistic activity in a dose-dependent manner. In contrast, N7, in addition to mutTNF, barely displays any agonistic activity (Fig. A). Moreover, N7 had an almost identical antagonistic activity for TNFR1-mediated bioactivity to that of mutTNF (Fig. B). Next, TNFR2-mediated activities of these TNFR1-selective antagonists were measured using hTNFR2/mFas-preadipocyte cells. The bioactivity of mutTNF and N7 via TNFR2 was much lower than that of wtTNF. Remarkably, TNFR2-mediated agonistic activity of N7 was lower than that of mutTNF, in agreement with the reduced affinity for TNFR2 (Fig. C).

In conclusion, we have succeeded in creating a TNFR1-selective antagonist with improved TNFR1-selectivity over that of mutTNF. This was achieved by constructing a library of mutTNF variants using a phage display technique. While TNFR1 is believed to be important for immunological responses (Rothe et al. 1993), TNFR2 is thought to be important for antiviral resistance and is effective for controlling mycobacterial infection by affecting membrane-bound TNF stimulation (Saunders et al. 2005; Olleros et al. 2002). Therefore, use of N7 might reduce the risk of side effects, such as infections, when applying TNF blockade as a therapy for autoimmune disease. We are currently evaluating the therapeutic effect of N7 using a mouse autoimmune disease model.

3. Experimental

3.1. Cell culture

HEp-2 cells (a human fibroblast cell line) were provided by Cell Resource Center for Biomedical Research (Tohoku University, Sendai) and were maintained in RPMI 1640 medium supplemented with 10% FBS and 1% antibiotics cocktail (penicillin 10,000 units/ml, streptomycin 10 mg/ml, and amphotericin B 25 µg/ml). L-M cells (a mouse fibroblast cell line) were provided by Mochida Pharmaceutical Co. Ltd. (Tokyo, Japan) and were maintained in minimum Eagle's medium supplemented with 1% FBS and 1% antibiotics cocktail. hTNFR2/mFas-preadipocyte cells were established previously in our laboratory (Abe et al. 2008) and were maintained in Dulbecco's modified Eagle's medium supplemented with Blastidicin S HCl, 10% FBS, 1 mM sodium pyruvate, 5×10^{-5} M 2-mercaptoethanol, and 1% antibiotic cocktail.

3.2. Construction of a novel gene library displaying mutTNF variants

The pCANTAB phagemid vector encoding mutTNF was used as template for PCR. The mutTNF was created in previous study and showed TNFR1-selective antagonistic activity (Shibata et al. 2008b). The six amino acid residues at the receptor binding site (amino acid residues; 29, 31, 32 and 145–147) of mutTNF were replaced with other amino acids using a 2-step PCR procedure as described previously (Mukai et al. 2009).

3.3. Selection of TNFR1-selective antagonist candidates from a mutTNF mutated phage library

Human TNFR1 Fc chimera (R&D systems, Minneapolis, MN) was immobilized onto a CM3 sensor chip as described previously. Briefly, the phage display library (1×10^{11} CFU/100 µl) was injected over the sensor chip at a flow rate of 3 µl/min. After binding, the sensor chip was washed using the rinse command until the association phase was reached. Elution was carried out using 4 µl of 10 mM glycine-HCl. The eluted phage pool was neutralized with 1 M Tris-HCl (pH 6.9) and then used to infect *E. coli* TG1 in order to amplify the phage. The panning steps were repeated twice. Subsequently, single clones were isolated and supernatant from each clone was collected and used to determine the cytotoxicity in the HEp-2 cytotoxic assay and the affinity for TNFR1 by ELISA, respectively

(Shibata et al. 2008b). We screened clones having almost no cytotoxicity but significant affinity for TNFR1. The phagemids purified from single clones were sequenced using the Big Dye Terminator v3.1 kit (Applied Biosystems, Foster City, CA). Sequencing reactions were analyzed on an ABI PRISM 3100 (Applied Biosystems).

3.4. Surface plasmon resonance assay (BIAcore® assay)

The binding kinetics of the proteins were analyzed by the surface plasmon resonance technique by BIAcore® (GE Healthcare, Amersham, UK). Each TNF receptor was immobilized onto a CM5 sensor chip, which resulted in an increase of 3,000–3,500 resonance units. During the association phase, all clones serially diluted in running buffer (HBS-EP) were allowed to pass over TNFR1 and TNFR2 at a flow rate of 20 µl/min. Kinetic parameters for each candidate were calculated from the respective sensorgram using BIAevaluation 4.0 software.

3.5. Cytotoxicity assay

In order to measure TNFR1-mediated cytotoxicity, HEp-2 or L-M cells were cultured in 96-well plates in the presence of TNF mutants and serially diluted wtTNF (Peptotech, Rocky Hill, NJ) with 100 µg/ml cycloheximide for 18 h at 4×10^4 cells/well or for 48 h at 1×10^4 cells/well. Cytotoxicity was then assessed using the methylene blue assay as described previously (Mukai et al. 2009; Shibata et al. 2004). For the TNFR1-mediated antagonistic assay, cells were cultured in the presence of 5 ng/ml human wtTNF and a serial dilution of the mutTNF. For the TNFR2-mediated cytotoxic assay, hTNFR2/mFas-preadipocyte cells were cultured in 96-well plates in the presence of TNF mutants and serially diluted wtTNF (1×10^4 cells/well) (Abe et al. 2008). After incubation for 48 h, cell survival was determined using the methylene blue assay.

Acknowledgement: This study was supported in part by Grants-in-Aid for Scientific Research from the Ministry of Education, Culture, Sports, Science and Technology of Japan, and by Grants-in-Aid for Scientific Research from Japan Society for the Promotion of Science (JSPS). In addition, this study was also supported in part by Health Labour Sciences Research Grants from the Ministry of Health, Labor and Welfare of Japan, Health Sciences Research Grants for Research on Publicly Essential Drugs and Medical Devices from the Japan Health Sciences Foundation and by a Grant from the Minister of the Environment, as well as THE NAGAI FOUNDATION TOKYO.

References

- Abe Y, Yoshikawa T, Kamada H, Shibata H, Nomura T, Minowa K, Kayamuro H, Katayama K, Miyoshi H, Mukai Y, Yoshioka Y, Nakagawa S, Tsunoda S, Tsutsumi Y (2008) Simple and highly sensitive assay system for TNFR2-mediated soluble- and transmembrane-TNF activity. *J Immunol Methods* 335: 71–78.
- Aggarwal BB (2003) Signalling pathways of the TNF superfamily: a double-edged sword. *Nat Rev Immunol* 3: 745–756.
- Brown SL, Greene MH, Gershon SK, Edwards ET, Braun MM (2002) Tumor necrosis factor antagonist therapy and lymphoma development: twenty-six cases reported to the Food and Drug Administration. *Arthritis Rheum* 46: 3151–3158.
- Feldmann M (2002) Development of anti-TNF therapy for rheumatoid arthritis. *Nat Rev Immunol* 2: 364–371.
- Goldbach-Mansky R, Lipsky PE (2003) New concepts in the treatment of rheumatoid arthritis. *Annu Rev Med* 54: 197–216.
- Gomez-Reino JJ, Carmona L, Valverde VR, Mola EM, Montero MD (2003) Treatment of rheumatoid arthritis with tumor necrosis factor inhibitors may predispose to significant increase in tuberculosis risk: a multicenter active-surveillance report. *Arthritis Rheum* 48: 2122–2127.
- Grell M, Becke FM, Wajant H, Mannel DN, Scheurich P (1998) TNF receptor type 2 mediates thymocyte proliferation independently of TNF receptor type 1. *Eur J Immunol* 28: 257–263.
- Imai S, Mukai Y, Takeda T, Abe Y, Nagano K, Kamada H, Nakagawa S, Tsunoda S, Tsutsumi Y (2008) Effect of protein properties on display efficiency using the M13 phage display system. *Pharmazie* 63: 760–764.
- Kim EY, Priatel JJ, Teh SJ, Teh HS (2006) TNF receptor type 2 (p75) functions as a costimulator for antigen-driven T cell responses *in vivo*. *J Immunol* 176: 1026–1035.
- Kim EY, Teh HS (2001) TNF type 2 receptor (p75) lowers the threshold of T cell activation. *J Immunol* 167: 6812–6820.
- Kollias G, Kontoyiannis D (2002) Role of TNF/TNFR in autoimmunity: specific TNF receptor blockade may be advantageous to anti-TNF treatments. *Cytokine Growth Factor Rev* 13: 315–321.

- Lubel JS, Testro AG, Angus PW (2007) Hepatitis B virus reactivation following immunosuppressive therapy: guidelines for prevention and management. *Intern Med J* 37: 705–712.
- Mori L, Iselin S, De Libero G, Lesslauer W (1996) Attenuation of collagen-induced arthritis in 55-kDa TNF receptor type 1 (TNFR1)-IgG1-treated and TNFR1-deficient mice. *J Immunol* 157: 3178–3182.
- Mukai Y, Shibata H, Nakamura T, Yoshioka Y, Abe Y, Nomura T, Taniai M, Ohta T, Ikemizu S, Nakagawa S, Tsunoda S, Kamada H, Yamagata Y, Tsutsumi Y (2009) Structure-function relationship of tumor necrosis factor (TNF) and its receptor interaction based on 3D structural analysis of a fully active TNFR1-selective TNF mutant. *J Mol Biol* 385: 1221–1229.
- Nagano K, Imai S, Mukai Y, Nakagawa S, Abe Y, Kamada H, Tsunoda S, Tsutsumi Y (2009) Rapid isolation of intrabody candidates by using an optimized non-immune phage antibody library. *Pharmazie* 64: 238–241.
- Nomura T, Kawamura M, Shibata H, Abe Y, Ohkawa A, Mukai Y, Sugita T, Imai S, Nagano K, Okamoto T, Tsutsumi Y, Kamada H, Nakagawa S, Tsunoda S (2007) Creation of a novel cell penetrating peptide, using a random 18mer peptides library. *Pharmazie* 62: 569–573.
- Olleros ML, Guler R, Corazza N, Vesin D, Eugster HP, Marchal G, Chavarot P, Mueller C, Garcia I (2002) Transmembrane TNF induces an efficient cell-mediated immunity and resistance to *Mycobacterium bovis* bacillus Calmette-Guerin infection in the absence of secreted TNF and lymphotoxin-alpha. *J Immunol* 168: 3394–3401.
- Rothe J, Lesslauer W, Lotscher H, Lang Y, Koebel P, Kontgen F, Althage A, Zinkernagel R, Steinmetz M, Bluethmann H (1993) Mice lacking the tumour necrosis factor receptor 1 are resistant to TNF-mediated toxicity but highly susceptible to infection by *Listeria monocytogenes*. *Nature* 364: 798–802.
- Saunders BM, Tran S, Ruuls S, Sedgwick JD, Briscoe H, Britton WJ (2005) Transmembrane TNF is sufficient to initiate cell migration and granuloma formation and provide acute, but not long-term, control of *Mycobacterium tuberculosis* infection. *J Immunol* 174: 4852–4859.
- Shibata H, Yoshioka Y, Ikemizu S, Kobayashi K, Yamamoto Y, Mukai Y, Okamoto T, Taniai M, Kawamura M, Abe Y, Nakagawa S, Hayakawa T, Nagata S, Yamagata Y, Mayumi T, Kamada H, Tsutsumi Y (2004) Functionalization of tumor necrosis factor-alpha using phage display technique and PEGylation improves its antitumor therapeutic window. *Clin Cancer Res* 10: 8293–8300.
- Shibata H, Yoshioka Y, Ohkawa A, Abe Y, Nomura T, Mukai Y, Nakagawa S, Taniai M, Ohta T, Mayumi T, Kamada H, Tsunoda S, Tsutsumi Y (2008a) The therapeutic effect of TNFR1-selective antagonistic mutant TNF-alpha in murine hepatitis models. *Cytokine* 44: 229–233.
- Shibata H, Yoshioka Y, Ohkawa A, Minowa K, Mukai Y, Abe Y, Taniai M, Nomura T, Kayamuro H, Nabeshi H, Sugita T, Imai S, Nagano K, Yoshikawa T, Fujita T, Nakagawa S, Yamamoto A, Ohta T, Hayakawa T, Mayumi T, Vandenabeele P, Aggarwal BB, Nakamura T, Yamagata Y, Tsunoda S, Kamada H, Tsutsumi Y (2008b) Creation and X-ray structure analysis of the tumor necrosis factor receptor-1-selective mutant of a tumor necrosis factor-alpha antagonist. *J Biol Chem* 283: 998–1007.
- Yamamoto Y, Tsutsumi Y, Yoshioka Y, Nishibata T, Kobayashi K, Okamoto T, Mukai Y, Shimizu T, Nakagawa S, Nagata S, Mayumi T (2003) Site-specific PEGylation of a lysine-deficient TNF-alpha with full bioactivity. *Nat Biotechnol* 21: 546–552.

疾患プロテオミクスからバイオマーカーの創出へ
—抗体プロテオミクス技術の確立とがん関連マーカーの探索—

長野一也,^a 今井 直,^a 中川晋作,^{b,c} 角田慎一,^{*,a,b,c} 堤 康央^{a,b,c}

From Disease Proteomics to Biomarker Development
—Establishment of Antibody Proteomics Technology and
Exploration of Cancer-related Biomarkers—

Kazuya NAGANO,^a Sunao IMAI,^a Shinsaku NAKAGAWA,^{b,c}
Shin-ichi TSUNODA,^{*,a,b,c} and Yasuo TSUTSUMI^{a,b,c}

^aLaboratory of Pharmaceutical Proteomics (LPP), National Institute of Biomedical Innovation (NiBio),
7-6-8 Saito-Asagi, Ibaraki, Osaka 567-0085, Japan, ^bGraduate School of Pharmaceutical Sciences,
Osaka University, 1-6 Yamadaoka, Suita, Osaka 565-0871, Japan, and ^cThe Center for
Advanced Medical Engineering and Informatics, Osaka University,
2-2 Yamadaoka, Suita, Osaka 565-0871, Japan

(Received August 31, 2009)

Molecular biomarkers are keys to the development of new diagnostic protocols and therapies. Recently, significant research effort has been devoted to the development of these biomarkers using various approaches. Perhaps the most promising approach is disease proteomics. This method involves analyzing and identifying changes in the expression pattern at the protein level in the diseased condition (disease-related proteins) by using two-dimensional differential gel electrophoresis analysis (2D-DIGE). In the case of disease proteomics, hundreds of candidate disease-related proteins can be identified at a time. Therefore, how to pick the really valuable proteins up from a number of candidate drug targets is the most important issue to be solved worldwide. Here, we introduce a novel approach, termed “antibody proteomics”, which addresses this issue. Using antibody proteomics it is possible to identify a variety of disease-related proteins by 2D-DIGE and simultaneously prepare monoclonal antibodies to these proteins by using a phage antibody library. The advantage of this technology is that the target proteins are identified in a high-throughput manner. Our approach relies on the fact that tissue microarray analysis can evaluate the relationship between disease-related proteins and disease progression, based on clinical and pathological information. In this review, we discussed the development and application of antibody proteomics and gave an overview of future work.

Key words—antibody proteomics; molecular biomarker; disease proteomics; phage antibody library

1. はじめに

近年のプロテオミクス関連技術の進展に伴って、がんを始めとする各種病態を的確に診断するための“疾患バイオマーカー”や“創薬ターゲットあるいは医薬品シーズ”等を探索し、医薬品開発への展開を目指す創薬プロテオミクス研究に大きな期待が寄

せられ、熾烈な国際的競争が繰り広げられている。¹⁾ 欧米各国では既に、2000年頃から大量の国家予算を投じ、メガファーマやバイオベンチャーをも巻き込んで、創薬プロテオミクス研究に大規模着手しており、本邦でも厚生労働省所管の国家プロジェクト等により現在研究が推進されているところである。しかし残念ながら、世界的にみても、創薬プロテオミクス研究から医薬品開発にまで展開できた例はいまだ乏しいのが現状である。それは、疾患の発症や悪化の際には数十から数百種類以上ものタンパク質が発現変動しており、これらの中から本当に価値のある『疾患バイオマーカーや創薬ターゲット/医薬品シーズ』の候補となるタンパク質を絞り込む

^a独立行政法人医薬基盤研究所創薬プロテオミクスプロジェクト(〒567-0085 大阪府茨木市彩都あさぎ7-6-8),

^b大阪大学大学院薬学研究科(〒565-0871 大阪府吹田市山田丘1-6), ^c大阪大学臨床医工学融合研究教育センター(〒565-0871 大阪府吹田市山田丘2-2)

*e-mail: tsunoda@nibio.go.jp

本総説は、日本薬学会第129年会シンポジウムGS6で発表したものを中心に記述したものである。

プロセスが不可欠であるが、それを可能とする技術基盤が圧倒的に不足していることに起因している。有用な候補タンパク質を絞り込むには、数多くの発現変動タンパク質の機能・局在、及び病態との関連解析が必要であり、そのためのツールとして、個々のタンパク質に対するモノクローナル抗体を得ることが必須である。しかし、抗体作製には、わずか一種類のタンパク質に対してですら、組換えタンパク質の作製、マウス等の動物への免疫、ハイブリドーマの作製とスクリーニング等のステップが必要であり、半年から数年を要してしまうため、プロテオミクスで見い出される数十から数百種類以上もの候補タンパク質に対してモノクローナル抗体を作製することは不可能といってもよい。これは、プロテオミクス研究に限らず、ゲノミクス・トランスクリプトミクスといった創薬を志向したオミクス研究全般に当てはまることであり、オミクス創薬のスループットを大きく制限する要因となっている。また、抗体創製の課題を克服できたとしても、『疾患バイオマーカーや創薬ターゲット/医薬品シーズ』の候補タンパク質が絞り込まれた後には、多数の臨床検体を用いて、候補タンパク質の発現と病態との関連をバリデーションしなければならない。しかし、このバリデーションのプロセスに関しても、膨大な数の臨床検体に対して、時間と労力を消費しながら解析せざるを得ないのが現状である。したがって、上記問題を克服し、創薬バイオマーカータンパク質を効率よく絞り込み、バリデーションを行って得る基盤技術の確立は、わが国の現在及び今後の創薬研究にとって緊急の課題である。

本観点から筆者らは、上記課題を克服し、創薬バイオマーカータンパク質を効率よく絞り込み、バリデーションを行って得る創薬基盤技術、「抗体プロテオミクス技術」を確立し、疾患マーカーや創薬ターゲットタンパク質の探索を進めている。本稿では、抗体プロテオミクス技術による乳がん関連バイオマーカータンパク質の探索の試みについて紹介する。

2. 抗体プロテオミクス技術

プロテオミクスによる発現変動タンパク質の網羅的探索には、2次元ディファレンシャル電気泳動(2D-DIGE)解析が汎用されている。そこで、2D-DIGE解析から同定・回収される微量で多種類の発現変動タンパク質に対して、網羅的なモノクローナ

ル抗体の創製を実現するため、*in vitro*で抗体を作製可能なファージ抗体ライブラリに着目した。筆者らは、これまで独自にノウハウを確立してきたファージ表面提示法を駆使することにより、^{2,3)}理論上あらゆる抗原に対する抗体を含んだナイーブファージ抗体ライブラリを独自に開発し、様々な抗原タンパク質に対して、最短2週間でモノクローナル抗体を作製することに成功している。⁴⁾また、微量抗原からでも抗体を単離できるように、抗原タンパク質の固相担体として、タンパク質の吸着能に優れるニトロセルロース膜を用いたファージ抗体ライブラリの濃縮法(メンブランパンニング法)を開発した。本方法を用いることで、わずか0.5 ngのタンパク質を得ることができれば、目的のファージ抗体を単離可能となった。一方で筆者らは、もう一つの課題であった候補タンパク質のバリデーション法に対して、組織マイクロアレイを用いた発現プロファイリングに着目した。組織マイクロアレイとは、多数の臨床組織切片を1枚のスライドガラス上に搭載したものであり、抗体を用いて免疫染色を行うことにより、目的タンパク質の発現プロファイルを一挙に取得でき、さらに各症例にリンクした種々の臨床情報との相関解析が可能である。

以上、疾患サンプルの2D-DIGE法による発現変動タンパク質の同定から、抗体作製と多数の臨床サンプルでのバリデーションまでのプロセスを、迅速かつ効率よく完了できるシステムを「抗体プロテオミクス技術」と称している。具体的なプロセスとしては、Fig. 1で示すように、①疾患サンプルとしてがん細胞株等を用い、健常組織由来細胞株を対照として、2D-DIGEにより発現変動タンパク質を探索する。②電気泳動後のゲルから回収される数100 ng以下のタンパク質の一部を使用して質量分析法によりタンパク質を同定する。③一方で、一部のタンパク質をニトロセルロース膜上に固相化し、24億種類の抗体レパートリーからなるナイーブファージ抗体ライブラリにより、目的とするタンパク質に対して高親和性抗体クローンをスクリーニングする。④得られたファージ抗体と組織マイクロアレイによる発現プロファイリングにより、多数の臨床サンプルでのバリデーションを行う。本技術は、多数の発現変動タンパク質の中から本当に価値のある『疾患バイオマーカーや創薬ターゲット』の候補を、効率

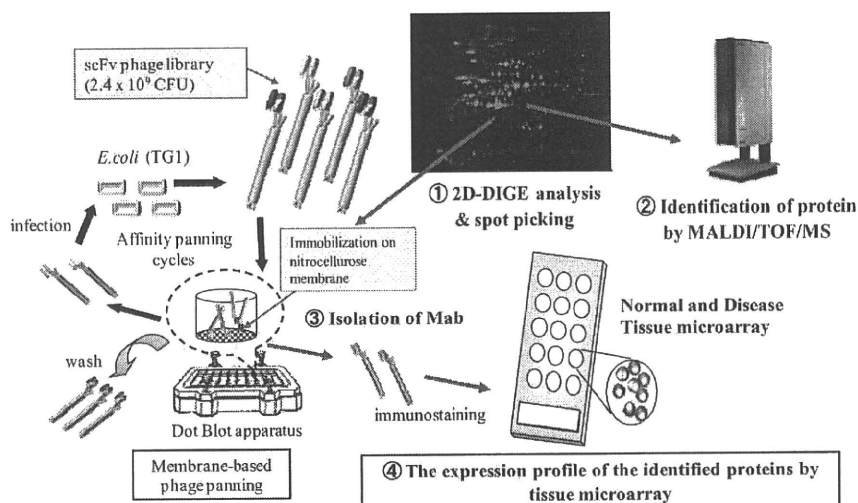


Fig. 1. Schematic Illustration of Antibody Proteomics Technology

Monoclonal antibodies against many differentially expressed proteins could be rapidly created by applying naive phage scFv library to proteomics study, and these candidates could be effectively validated by tissue microarray.

よく絞り込み・バリデーションできる唯一の方法であり、創薬プロテオミクス研究に極めて有用な基盤技術になるものと考えられる。

そこで以下に、本技術の有用性評価を目的として、乳がんの創薬ターゲットタンパク質、あるいは悪性度診断のためのマーカータンパク質の同定を試みた。

3. プロテオーム解析による乳がん関連タンパク質の同定と網羅的な抗体作製

不死化乳腺細胞株 184A1 から調製したタンパク質を対照サンプルに、乳がん細胞株 SKBR3 から調製したタンパク質を疾患サンプルとして 2次元ディファレンシャル電気泳動 (2D-DIGE) 解析を行った。定量的解析により発現変動レベルの大きかった 21 個の spot について、ゲルを切り出し、ゲルを溶解することによりタンパク質を回収した。回収したタンパク質の一部を用いて質量分析 (MS) により解析 (PMF 及び MS/MS) したところ、すべてのスポットのタンパク質を同定することができた (Table 1)。また、回収したタンパク質の一部を用いて、メンブランパンニング法によりファージ抗体の単離を試みた。その結果、21 種類すべてのタンパク質に対して親和性を有するファージ抗体を単離することができた。ファージ抗体の単離に要した時間は約 2 週間であり、2D-DIGE によるプロテオーム解析から同定・回収される微量で多種類のタンパク質を直接抗原として使用し、それらに対する抗体

Table 1. Identification of Differentially Expressed Proteins in Breast Cancer Cells by MALDI-TOF/MS

spot	protein name	MW	pI	cancer/normal
# 1	splicing factor YT521-B isoform 1	84649	5.9	Up 6-fold
# 2	IkappaBR	62872	5.5	Up 6-fold
# 3	SPATA5 protein	75580	5.6	Up 7-fold
# 4	skin aspartic protease	36938	5.3	Down 11-fold
# 5	beta actin variant	41694	5.3	Up 15-fold
# 6	TRAIL-R2	47820	5.4	Up 18-fold
# 7	cytokeratin 18	47305	5.3	Up 12-fold
# 8	TRAIL-R2 (Death receptor 5)	47820	5.4	Up 16-fold
# 9	RREB1 protein	51563	5.3	Up 10-fold
# 10	keratin K7 type II epithelial	51333	5.4	Up 23-fold
# 11	keratin 18	48029	5.3	Up 13-fold
# 12	keratin K7 type II epithelial	51333	5.4	Up 24-fold
# 13	FLJ31438 protein	52992	5.5	Up 35-fold
# 14	Keratin type II cytokeletal 7	51312	5.5	Up 36-fold
# 15	hPAK65	54880	5.7	Up 8-fold
# 16	Cytokeratin 8	53529	5.5	Up 32-fold
# 17	Keratin type II cytokeletal 8	53540	5.5	Up 72-fold
# 18	XRN1 protein	53784	5.8	Up 8-fold
# 19	Jerky protein homolog-like	50678	6.0	Up 22-fold
# 20	EPH receptor A10	32130	5.7	Up 9-fold
# 21	glutathione transferase	23159	5.4	Down 53-fold

を迅速に取得可能な方法論であることが確認できた。

4. 組織マイクロアレイ解析を用いた乳がん関連マーカータンパク質の探索

タンパク質に対する抗体を手にすることができれば、様々な機能解析が可能となる。そこで、得られ

たファージ抗体を用いて、がん組織アレイの免疫染色を行い、同定されたタンパク質の発現プロファイリングを試みた。189 症例の乳がん組織と 15 症例の正常の乳腺組織が搭載された組織マイクロアレイを用いて、ファージ抗体にて染色した。その結果、SPATA5 protein, Beta actin variant, FLJ31438 protein, HPAK65, XRN1 protein に関しては正常乳腺組織においても、がん組織においてもほとんど発現は認められなかった。一方、EPH receptor A10 (EPHA10) は約 50%, TRAIL-R2 は約 60%, Cytokeratin 8 は約 70% の症例で高発現しており、一方で正常乳房組織での発現は認められなかった (Table 2)。現在、乳がんマーカーとして臨床で汎用されている Her-2 が約 30% の陽性率であることを考慮すると、これら 3 種類のタンパク質は、乳がんの優れた創薬ターゲットになり得るものと期待される。また、Her-2 陽性あるいは陰性症例において、これら候補タンパク質発現を調べたところ、Her-2 陽性患者のうち、TRAIL-R2 あるいは EPHA10 は、約 77% あるいは 62% の割合で発現しており、両者の発現を合わせると約 87% の症例で発現していた。一方、Her-2 陰性の症例においても、約 70% の症例が TRAIL-R2 あるいは EPHA10 いずれかに陽性であった [Fig. 2(A)]。現在臨床で、Trastuzumab (Her-2 を標的とした抗体医薬) が乳がんに対する画期的な抗体医薬として汎用されているが、TRAIL-R2 と EPHA10 も細胞膜タンパク質

であることから、Trastuzumab が無効な症例に対する新規治療標的になり得るものと期待される。また、Her-2 陽性症例においても、Trastuzumab による治療を続けるうちに耐性が生じることが問題になっていることから、⁵⁻⁷⁾ そのような患者に対しても有効な治療標的になり得るものと期待される。

続いて、上記候補分子の発現と病期との相関を解析したところ、Cytokeratin 8 と EPHA10 の発現は乳がんの病期の進行と有意な相関が認められた [Fig. 2(B)]。したがって、Cytokeratin 8 や EPHA10 は乳がんの進行に関連するタンパク質であり、悪性度を客観的に予測・評価し得る診断マーカーになり得るものと考えられる。

近年、TRAIL-R2 は、がんの新たな分子標的として抗体医薬の開発が進んでおり、⁸⁻¹⁰⁾ また Cytokeratin 8 はがんの悪性度に係ることが報告されている。¹¹⁻¹³⁾ 以上の結果は、抗体プロテオミクス技術が、多種類の発現変動タンパク質の中から、有用なマーカータンパク質を迅速かつ効率的に絞り込むことが可能な極めて有用な創薬基盤技術であることを示すものである。

5. おわりに

本稿では、われわれが確立した『抗体プロテオミクス技術』によって、迅速に創薬バイオマーカータンパク質の候補として、TRAIL-R2, Cytokeratin 8, EPHA10 を絞り込むことができた。中でも TRAIL-R2, EPHA10 は、既存の乳がんマーカータンパク質 Her-2 に替わる新たな創薬ターゲットタンパク質になり得ることが示唆された。現在、これら分子に対するより詳細な機能解析を進めるとともに、抗体医薬の開発を目指して研究を行っている。今後、抗体プロテオミクス技術が、世界に遅れをとるわが国の抗体医薬等の創薬研究に貢献することを願っている。

謝辞 本研究を遂行するにあたり、組織マイクロアレイ解析の御指導を賜りました富山大学医学部附属病院・福岡順也博士に感謝の意を表します。なお本研究では、文部科学省科学研究費補助金特定領域研究 (No. 20015052)、日本学術振興会科学研究費補助金基盤研究 B 一般 (No. 21390046)、厚生労働科学研究費補助金医薬品・医療機器等レギュラトリーサイエンス総合研究事業 (No. H19-医薬一般

Table 2. Validation of Biomarker Candidates by Tissue Microarray with Breast Tumor and Breast Normal Tissues

protein name	positive rate of various antigens	
	normal tissue	breast cancer tissue
Her-2	0/15 (0%)	53/189 (28.0%)
IkappaBR	3/15 (20.0%)	22/189 (11.6%)
SPATA5 protein	0/15 (0%)	0/189 (0%)
Beta actin variant	0/15 (0%)	0/189 (0%)
TRAIL-R2	0/15 (0%)	119/189 (63.0%)
RREB-1	1/15 (6.7%)	83/189 (43.9%)
FLJ31438 protein	0/15 (0%)	0/189 (0%)
HPAK65	0/15 (0%)	0/189 (0%)
Cytokeratin 8	0/15 (0%)	137/189 (72.5%)
XRN1 protein	0/15 (0%)	0/189 (0%)
Jerky protein homolog-like	0/15 (0%)	0/189 (0%)
EPHA10	0/15 (0%)	93/189 (49.2%)

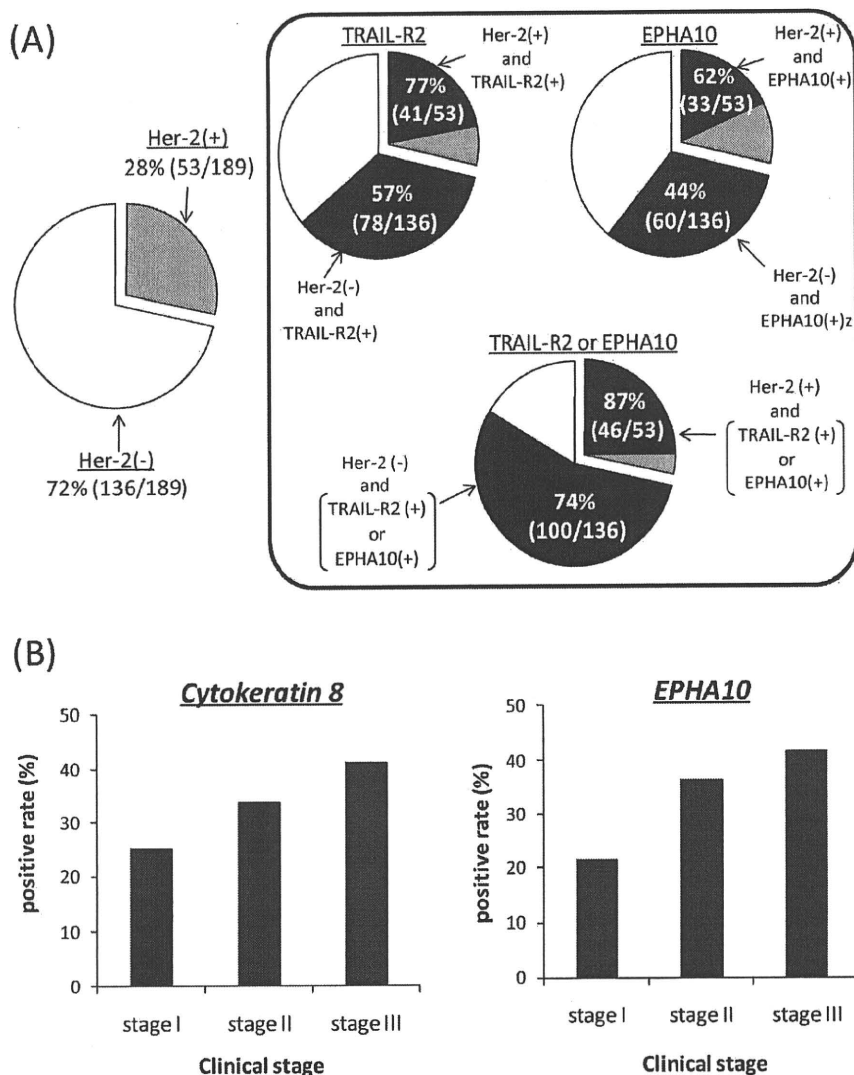


Fig. 2. Correlation Analysis between the Expression Profile of Biomarker Candidates and Clinical Information

(A) The expression rate of drug target candidates, TRAIL-R2 and EPHA10, in Her-2 positive and negative cases. The expression of Her-2 in 28% of breast tumor cases describes gray. The expression of each candidate in Her-2 positive and negative cases describes black. (B) The expression rate of diagnosis marker candidates, Cytokeratin8 and EPHA10, in each clinical stage.

-010), 厚生労働科学研究費補助金政策創薬総合研究 (HS) 事業 (No.KHC1017), 厚生労働科学研究費補助金創薬基盤推進研究事業: 創薬バイオマーカー探索研究事業 (No.H21-バイオ-指定-005), 及び財団法人永井記念薬学国際交流財団の支援を受けて実施されたものです。ここに深謝申し上げます。

REFERENCES

- 1) Hanash S., *Nature*, **422**, 226-232 (2003).
- 2) Yamamoto Y., Tsutsumi Y., Yoshioka Y., Nishibata T., Kobayashi K., Okamoto T., Mukai Y., Shimizu T., Nakagawa S., Nagata S., Mayumi T., *Nat. Biotechnol.*, **21**, 546-552 (2003).
- 3) Shibata H., Yoshioka Y., Ohkawa A., Minowa K., Mukai Y., Abe Y., Tani M., Nomura T., Kayamuro H., Nabeshi H., Sugita T., Imai S., Nagano K., Yoshikawa T., Fujita T., Nakagawa S., Yamamoto A., Ohta T., Hayakawa T., Mayumi T., Vandenberg P., Aggarwal B. B., Nakamura T., Yamagata Y., Tsunoda S., Kamada H., Tsutsumi Y., *J. Biol. Chem.*, **283**, 998-1007, (2008).
- 4) Imai S., Mukai Y., Nagano K., Shibata H., Sugita T., Abe Y., Nomura T., Tsutsumi Y.,